

Cross-Over Between First-Order and Critical Wetting at the Liquid-Vapour Interface of *n*-Alkane/Methanol Mixtures: Tricritical Wetting and Critical Prewetting

A. I. Posazhennikova,¹ J. O. Indekeu,¹ D. Ross,² D. Bonn,³ and J. Meunier³

Received November 6, 2001; revised May 27, 2002

A simple mean-field theory is presented which describes the basic observations of recent experiments revealing rich wetting behaviour of *n*-alkane/methanol mixtures at the liquid-vapour interface. The theory, qualitative and in part heuristic, is based on a microscopic lattice-gas model from which a Cahn–Landau approach is distilled. Besides the physics associated with the short-range components of the intermolecular interactions, effects of the long-range tails of the net van der Waals forces between interfaces are also taken into account. Further, gravitational thinning of the wetting phase is incorporated. The calculation of the spreading coefficient S is extended to the experimentally relevant situation in which the bulk adsorbate is slightly away from two-phase coexistence due to gravity. Analysis of this novel approximation to S for systems with short-range forces leads to the conclusion that the surface specific heat exponents $\alpha_s = 1, 1/2,$ and 0 , for first-order wetting, tricritical wetting and critical wetting, respectively, are robust with respect to (weak) gravitational thinning, consistently with experiment. For three different systems the adsorption is calculated as a function of temperature and compared with the experimentally measured ellipticity. Including weak long-range forces which favour wetting in the theory does not visibly alter the critical wetting transition for the nonane/methanol mixture, in contrast with the generic expectation of first-order wetting for such systems, but in good agreement with experiment. For decane/methanol

¹Laboratorium voor Vaste-Stoffysica en Magnetisme, Katholieke Universiteit Leuven, B-3001 Leuven, Belgium; e-mail: joseph.indekeu@fys.kuleuven.ac.be

²Process Measurements, National Institute of Standards and Technology, Gaithersburg, Maryland 20899.

³Laboratoire de Physique Statistique, Ecole Normale Supérieure, F-75231 Paris cedex 05, France.

weak long-range forces bring the transition very close to the prewetting critical point, leading to an adsorption behaviour closely reminiscent of short-range tricritical wetting, observed experimentally for alkane chain length between 9.6 and 10. Finally, for undecane/methanol the transition is clearly of first order. First-order wetting is also seen in the experiment.

KEY WORDS: Wetting phase transitions; critical wetting; tricritical wetting; long-range forces; binary liquid mixtures; adsorption.

1. INTRODUCTION AND PERSPECTIVE

Recent experiments have shown that a binary liquid mixture of linear or “normal” alkane and methanol in equilibrium with their common vapour displays a first-order wetting transition if the wetting temperature T_w is well below the consolute-point temperature T_c and a “short-range critical wetting” transition if T_w is very close to $T_c^{(1,2)}$. The latter is the case for *n*-nonane and methanol. The “substrate” in these wetting experiments is the saturated vapour phase. A recent review covers various examples of experimentally observed first-order or continuous wetting transitions in liquid mixtures.⁽³⁾

The observation of short-range critical wetting in adsorbed binary liquid mixtures is surprising, to say the least. Indeed, due to the presence of van der Waals forces, which induce an algebraically decaying long-ranged surface-interface interaction favouring wetting, a first-order wetting transition should be expected.^(4-8,11) Alternatively, if the van der Waals forces oppose wetting, no wetting transition should occur, unless the leading van der Waals interaction amplitude changes sign at some temperature, resulting in “long-range critical wetting,”⁽⁸⁻¹²⁾ observed experimentally in pentane on water.⁽¹³⁾ However, within the experimentally accessible range of small film thicknesses (up to 100 Å) the van der Waals forces can be neglected compared to exponentially decaying mean-field (MF) and fluctuation-induced (FI) interactions.^(1,2) The range of the MF and FI interactions is determined by the bulk correlation length, which can become as large as the wavelength of visible light very close to the upper consolute point, at T_c , where the two fluid phases become identical.

The experiments, and in particular the measured value of the surface specific-heat exponent, agree with the predictions of the mean-field theory, and disagree strongly with renormalization-group predictions based on a capillary-wave model.⁽¹⁴⁻¹⁷⁾ Furthermore, Monte Carlo simulations of short-range critical wetting⁽¹⁸⁾ also disagree with the RG predictions⁽¹⁸⁾ but agree with the experiments. This behaviour can be understood in the light of

more sophisticated interface models^(19–21) which indicate that the critical region around the transition, in which deviations from MF behaviour show up for the surface specific heat exponent, is too small to be relevant for either experiment or simulation. In other words, mean-field theory should be an excellent description of simulations and experiments of critical wetting with short-ranged forces. The experimental observations of mean-field like behaviour are thus entirely in keeping with the latest RG work, since in particular the mass density difference between the wetting phase and the surrounding bulk phase stop the parallel correlation length from getting big enough to see fluctuation effects. We shall return in detail to the relevance of this mass density difference in what follows.

Our aim in this paper is to give a theoretical description of the cross-over between the regimes of first-order wetting and “short-range critical wetting” in this system, *which for purely short-range forces would occur via a tricritical wetting point.*⁽²²⁾ In view of the observed consistency between experiment and MF theory, and the predictions for the width of the critical region discussed above, we adopt the point of view of the classical theory of Cahn–Landau type. We include the van der Waals forces as a weak perturbation and also take into account the gravitational thinning of the wetting layer due to the difference in the mass densities of the liquid phases. We neglect thermal fluctuation effects, but incorporate the influence of the vicinity of bulk criticality at the MF level. That is, the divergence of the bulk correlation length is included in the theory, but with the MF value for the critical exponent. In this way, the interplay of wetting and critical adsorption is allowed for.

This paper is organized as follows. In Section 2 we present the microscopic lattice-gas model for the alkane/methanol/vapour system and derive the Ising model coupling constants and fields from the intermolecular and chemical potentials. In Section 3 we extract the continuum Cahn–Landau theory from the Ising model near the bulk critical point. In Section 4 we study wetting layer thicknesses, adsorptions, surface free energies, spreading coefficients and critical exponents for the regimes of first-order, tricritical and critical wetting within the model featuring only short range forces. The cross-over from first-order to critical wetting including long-range forces in the theory is investigated in Section 5. There we calculate the system parameters corresponding to nonane/methanol, decane/methanol and undecane/methanol and derive adsorptions and spreading coefficients assuming the long-range forces to be a weak perturbation. We compare our results with the experiments and investigate whether we can interpret them in terms of short-range tricritical wetting or, alternatively, in terms of prewetting criticality induced by long-range forces. In Section 6 we present our conclusions.

2. MICROSCOPIC LATTICE-GAS MODEL

In this section we adopt the philosophy of lattice-gas modeling which is often applied to binary alloys etc., as exemplified in the lectures of Yeomans.⁽²³⁾ We consider a nearest-neighbour spin-1 Ising model on a 3-dimensional simple cubic (SC) or face-centered cubic (FCC) lattice. The spin variable takes the value +1 (methanol molecule), -1 (alkane molecule) or 0 (vacancy). The methanol-rich phase sits at the bottom of the recipient, the alkane-rich phase is in the middle, and the vapour is on top.

Given that our entire approach is based at mean-field level it would be appropriate to start from a density-functional theory of a binary mixture with long-ranged fluid-fluid forces, as can be derived starting from this spin-1 model following the works of Dietrich and Latz⁽²⁴⁾ and Getta and Dietrich.⁽¹²⁾ However, the application of this theory to non-spherical molecules such as alkanes, and to polar molecules such as methanol, would only be a first approximation, so that the difficult calculations inherent in this approach would still not be sufficiently reliable. We therefore feel the necessity to propose a much simpler strategy to get a handle on the cross-over from first-order to continuous wetting in the presence of long-range forces.

We introduce pair interaction energies ϵ_{MM} for methanol-methanol, ϵ_{AA} for alkane-alkane, and ϵ_{AM} for alkane-methanol pairs at nearest-neighbour distance. The AA energy corresponds in a first approximation to the Lennard-Jones potential well depth for the nonpolar alkane molecules and the MM energy can be given either by the Lennard-Jones or, more appropriately, by the Stockmayer potential well depth for the polar methanol molecules.⁽²⁵⁾ Furthermore, we introduce the chemical potentials μ_M and μ_A for methanol and alkane particles, respectively. We make the rough approximation that a *single lattice constant* σ suffices for the model, while in reality the distances of closest approach, reflected, e.g., by Lennard-Jones diameters σ_{MM} and σ_{AA} can differ for methanol and alkane molecules. Further, we ignore the chain conformation of the *n*-alkanes and treat them effectively as *spheres*.

The spin-1 Ising model Hamiltonian reads

$$\mathcal{H}(s) = -J \sum_{\langle ij \rangle} s_i s_j - H \sum_i s_i - \Delta \sum_{\langle ij \rangle} (s_i s_j^2 + s_j s_i^2) - E \sum_{\langle ij \rangle} s_i^2 s_j^2 - M \sum_i s_i^2, \quad (2.1)$$

where the square brackets $\langle ij \rangle$ indicate that the sums are over nearest neighbours on the lattice. The Ising couplings can easily be determined from the pair energies and chemical potentials, considering the following

pairs: vacancy-vacancy, methanol-vacancy, alkane-vacancy, methanol-methanol, alkane-alkane and alkane-methanol. This leads to the relations

$$J = (\epsilon_{MM} + \epsilon_{AA} - 2\epsilon_{AM})/4 \quad (2.2)$$

$$H = (\mu_M - \mu_A)/2 \quad (2.3)$$

$$\Delta = (\epsilon_{MM} - \epsilon_{AA})/4 \quad (2.4)$$

$$E = (\epsilon_{MM} + \epsilon_{AA} + 2\epsilon_{AM})/4 \quad (2.5)$$

$$M = (\mu_A + \mu_M)/2 \quad (2.6)$$

Since the vapour phase is dilute and the liquid phases are dense, we make the very reasonable approximation that the liquid is free of vacancies and that the liquid-vapour interface is sharp. This allows us to map the spin-1 model onto a spin-1/2 model *with a free surface*. The vapour phase is thus replaced by an inert spectator phase and vacancies no longer play a role. Therefore, inside the adsorbate we have $s_i^2 = 1$ everywhere, and our model reduces to one with spin 1/2 and bulk Hamiltonian

$$\mathcal{H}_{\text{bulk}} = -J \sum_{\langle ij \rangle} s_i s_j - H \sum_i s_i - \Delta \sum_{\langle ij \rangle} (s_i + s_j) + \text{constant} \quad (2.7)$$

For a lattice with coordination number q ($q=6$ for SC and 12 for FCC) we can rewrite this and drop the irrelevant constant, so that

$$\mathcal{H}_{\text{bulk}} = -J \sum_{\langle ij \rangle} s_i s_j - H_{\text{bulk}} \sum_i s_i \quad (2.8)$$

where the bulk field is given by

$$H_{\text{bulk}} = H + q\Delta \quad (2.9)$$

Bulk two-phase coexistence between the alkane-rich and methanol-rich phases is reached for $H_{\text{bulk}} = 0$ in this model.

We now proceed to derive the surface contribution to the Hamiltonian, $\mathcal{H}_{\text{surf}}$. The surface layer of spins is different from layers in the bulk in that there are missing bonds. For the SC lattice there is 1 nearest neighbour missing per surface site and for FCC there are 4 missing bonds, assuming a (100) surface for simplicity. For a (111) surface there would be 3 missing bonds. This leads to the result, for the surface layer,

$$\mathcal{H}_{\text{surf}} = -J \sum_{\langle ij \rangle} s_i s_j - H_{\text{surf}} \sum_i s_i \quad (2.10)$$

where the surface field H_{surf} takes the form

$$H_{\text{surf}} = H_{\text{bulk}} - m\Delta \quad (2.11)$$

with $m = 1$ for the SC lattice, and $m = 4$ for the FCC lattice. At, or very close to, bulk coexistence $H_{\text{bulk}} \approx 0$ so that the surface field is governed by Δ . In particular, the surface preferentially adsorbs that species for which the pair binding energy is smallest (in absolute value), in order to minimize the energy increase due to broken bonds.

We can estimate the leading surface field contribution Δ as follows. For n -alkanes we inspect the liquid-gas critical temperatures T_c^{LG} and adopt the simple rule $\epsilon_{AA} = 0.75k_B T_c^{\text{LG}}$ for obtaining the Lennard-Jones potential well depth.⁽²⁵⁾ This leads to the following estimates, from n -pentane (C_5H_{12}) to n -undecane ($\text{C}_{11}\text{H}_{24}$): $\epsilon_{AA}/k_B = 353$ K (pentane), 380 K (hexane), 405 K (heptane), 427 K (octane), 446 K (nonane), 464 K (decane), 480 K (undecane). For the polar molecule methanol, either we can use the Lennard-Jones parameter derived using the same rule, which leads to $\epsilon_{MM}/k_B = 385$ K, or we can employ the Stockmayer potential parameter $\epsilon_{MM}^S/k_B = 417$ K,⁽²⁵⁾ which is more suitable for polar molecules. Using (2.4) we see that *the surface field changes sign* between hexane and heptane, when the Lennard-Jones parameter is used for methanol. On the other hand, the sign reversal of Δ occurs *between heptane and octane* when the Stockmayer parameter is adopted. Experimentally, for short chain length of alkane the alkane-rich phase is preferentially adsorbed at the vapour phase, while for long chain length the methanol-rich phase is preferred.^(1,2) This is in agreement with the microscopic model, which predicts $\Delta > 0$ for short alkanes. Experimentally, the reversal of preferential adsorption takes place (approximately) for octane, which agrees well with the theoretical prediction based on the Stockmayer potential parameter for methanol, which we will therefore use from now on.

3. CONTINUUM CAHN-LANDAU THEORY

In this section we apply the mean-field approximation to the Ising Hamiltonian derived in the previous section, and subsequently make the continuum approximation to obtain the Cahn–Landau theory. We follow closely the derivation of Maritan, Langie, and Indekeu,⁽²⁶⁾ valid for slowly varying concentration profiles and for temperatures close to the consolute point of the alkane/methanol mixture. Additionally, we take into account that the mixture is at, or close to, two-phase coexistence in bulk.

Let N be the number of cells in the lattice-gas representation of our system and F the free energy. We have $N = V/\sigma^3$, where V is the volume

and σ is the representative molecular diameter, which serves as the lattice constant. The temperature at the critical point of the binary liquid mixture, or *upper consolute point*, is denoted by T_c . We consider the reduced free energy density $f = F/(Nk_B T_c)$ as a function of the order parameter ϕ . In our system ϕ is the concentration difference of methanol and alkane in the mixture, $x_M - x_A$, minus the critical concentration difference, $x_{M,c} - x_{A,c}$. We have, from $F = U - TS$,

$$f(\phi) = u(\phi) - T\sigma(\phi)/T_c \quad (3.1)$$

with energy density

$$u(\phi) = -\phi^2/2 - h\phi + \text{constant} \quad (3.2)$$

where h stands for the reduced bulk field, $h = H_{\text{bulk}}/k_B T_c$. The entropy density, ⁽²⁶⁾ to 4th order in ϕ , is given by

$$\sigma(\phi) = \ln 2 - \phi^2/2 - \phi^4/12 \quad (3.3)$$

We obtain

$$f(\phi) = \text{constant} - h\phi - (1 - T/T_c) \phi^2/2 + T\phi^4/(12T_c) \quad (3.4)$$

Note that the model is symmetric with respect to the interchange of (h, ϕ) and $(-h, -\phi)$. This symmetry is approximately valid for binary liquid mixtures near T_c .

For $h = 0$ we obtain the order parameter value ϕ_b for bulk coexistence from $df/d\phi = 0$. This leads to $\phi_b = \pm \phi_0$, with, for $T/T_c \approx 1$,

$$\phi_0^2 = 3(1 - T/T_c) \quad (3.5)$$

The free energy near T_c can be rewritten as

$$f(\phi) = \text{constant} - h\phi + (\phi^2 - \phi_0^2)^2/12 \quad (3.6)$$

In general, ϕ_b is found by minimizing $f(\phi)$, and taking that solution of the cubic equation which has largest modulus. The other solutions, if real, correspond to metastable and saddle points. A bulk spinodal results when the latter two coincide.

The Cahn-Landau surface free-energy functional can be written in the form ^(22, 27)

$$\gamma[\phi] = \int_0^\infty dz \left\{ \frac{c^2}{4} \left(\frac{d\phi}{dz} \right)^2 + f(\phi(z)) \right\} - h_1 \phi_1 - g \frac{\phi_1^2}{2} \quad (3.7)$$

where $z \geq 0$ measures the vertical distance from the liquid-vapour interface downwards into the binary liquid mixture. The distance is in units of the lattice spacing, or representative molecular diameter, in the underlying microscopic model. The last two terms constitute a surface contact energy which depends on the surface value of the order parameter, $\phi_1 = \phi(z=0)$, and will be discussed later. We remark that this functional gives only the surface free energy *excess* with respect to a reference value γ_0 that is independent of ϕ , but depends on the temperature and the material parameters of substrate and adsorbate. Therefore, the functional $\gamma[\phi]$ does not fulfill, for example, the positivity requirement of interfacial tensions in general. Since we will need to calculate only *differences* of surface free energies of substrate/adsorbate configurations, the unknown γ_0 drops out.

Having defined the function $f(\phi)$ previously, we now proceed to relate the coefficient of the gradient squared, $c^2/4$, to microscopic interaction energies and thermodynamic quantities. This was done in ref. 26 with the result

$$c^2/2 = J/k_B T_c \equiv K_c \quad (3.8)$$

For the 3-dimensional Ising model on the SC lattice, $K_c \approx 0.222$, while on the FCC lattice, $K_c \approx 0.102$. For comparison, the mean-field value for the critical reduced nearest-neighbour coupling is $K_c = 1/q$, where q is the coordination number. This gives $K_c = 0.167$ for SC, $K_c = 0.125$ for BCC, and $K_c = 0.083$ for FCC lattices, in the mean-field theory which we presently employ.

We now address the question whether we can estimate J theoretically. Therefore we turn to the microscopic equation (2.2) relating J to the molecular pair potentials. The “mixed” pair energy ϵ_{AM} is still to be determined. This is a non-trivial task, and we limit ourselves here to proposing reasonable arguments for obtaining a reliable order of magnitude. This exercise is without quantitative consequences for our theory, since we will not use this estimate further on, but will take experimental surface tension data as input for estimating J more reliably.

To proceed systematically we follow Israelachvili⁽²⁸⁾ and compare three classes of molecules: non-polar molecules interacting only through dispersion forces, polar molecules interacting through dispersion and dipolar forces, and polar molecules interacting also through hydrogen-bonding in addition to the other forces. For example, *ethane* (CH_3CH_3), *formaldehyde* (HCHO) and *methanol* (CH_3OH) have similar size and weight, but are non-polar, polar, and polar with H -bonds, respectively. The stronger is the interaction, the higher is the liquid-gas critical temperature of the pure component. For example, for ethane $T_c^{\text{LG}} = 305$ K, for formaldehyde the

dipole-dipole interaction leads to $T_c^{\text{LG}} = 408$ K, and additional hydrogen-bonding leads to $T_c^{\text{LG}} = 513$ K for methanol.

For unlike molecules within the same interaction class, the Lorentz–Berthelot combining rule,⁽²⁹⁾

$$\epsilon_{AB} = \sqrt{\epsilon_{AA}\epsilon_{BB}} \quad (3.9)$$

is often a reasonable approximation. However, for pairs composed of dissimilar molecules belonging to different classes, this rule can be a very poor approximation leading to ridiculously low estimates of the consolute-point temperature, especially when hydrogen-bonding occurs in one of the two components. The most dramatic manifestation of this “non-additivity” of interactions is the hydrophobic effect. When a non-polar component is mixed with water, the disruption of the hydrogen-bonded water network is so costly in energy that, instead of mixing, phase separation is likely to occur. In this case the mixed interaction strength ϵ_{AB} is smaller than either one of the pure values ϵ_{AA} or ϵ_{BB} , clearly violating (3.9).

We infer from this that a qualitatively similar phenomenon should occur when alkanes are mixed with methanol, the latter playing the role of water in the previous example. The network in this case consists of *one-dimensional chains*.⁽²⁸⁾ The mixed alkane-methanol interaction lacks the dipole-dipole and hydrogen-bonding contributions, and to a reasonable approximation one can say that an alkane molecule sees a methanol molecule as if it were a molecule of the same weight and size as methanol, but interacting only through dispersion forces. Therefore, for determining the mixed pair interaction, we make the rough approximation to replace methanol effectively by *ethane*, and then we apply the Lorentz–Berthelot rule. In doing so, we also neglect the dipole/induced-dipole contribution (induction force) to the mixed-pair van der Waals interaction. However, the induction force is usually small compared to the dispersion force.⁽²⁸⁾

For ethane, we estimate $\epsilon_{EE}/k_B = 0.75T_c^{\text{LG}}$, which gives 229 K. Using likewise the Lennard-Jones parameters for the other *n*-alkanes and adopting the rule (3.9) with ethane playing the role of methanol, this amounts to the following mixed pair parameters for alkane-methanol mixtures: $\epsilon_{AM}/k_B = 284$ K (pentane), 295 K (hexane), 305 K (heptane), 313 K (octane), 320 K (nonane), 326 K (decane), and 332 K (undecane). Now the nearest-neighbour couplings J can be determined, according to (2.2), with the results: $J/k_B = 50$ K (pentane), 52 K (hexane), 53 K (heptane), 55 K (octane), 56 K (nonane), 57 K (decane) and 58 K (undecane).

These values can be tested against the reported upper consolute temperatures T_c (at ambient pressure) for alkane-methanol mixtures,^(1,2) which are $T_c = 308$ K (hexane), 324 K (heptane), 340 K (octane), 352 K (nonane),

364 K (decane) and 376 K (undecane). The ratios $K_c = J/k_B T_c$ are, respectively, 0.169, 0.164, 0.162, 0.159, 0.157, and 0.154. These are very reasonable, since they lie in between the K_c -values for SC and FCC packings, and are very close to the mean-field value for the SC lattice. We conclude that the simple estimates we have made of the Ising model coupling J , based on approximate molecular pair energies, are consistent with the correct order of magnitude for the consolute-point temperatures of the binary mixtures and any reasonable choice of cubic lattice (FCC, BCC or SC) for the lattice in the model.

A more accurate procedure for determining the parameter c , or equivalently K_c , in (3.8) consists of comparing the experimentally measured liquid-liquid interfacial tension with the theoretical expression, derived within the Cahn–Landau theory (e.g., ref. 30),

$$\gamma_{MA} = c \int_{-\phi_0}^{\phi_0} d\phi \sqrt{f(\phi)} = 2c(1 - T/T_c)^{3/2} \quad (3.10)$$

The critical exponent $3/2$ is the mean-field value. In real fluids it is to be replaced by 1.26, and also the amplitude is to be modified. In order to obtain an estimate for the parameter c , we inspect published interfacial tension data for the nonane/methanol mixture by Carrillo *et al.*,⁽³¹⁾ for example. At $T = 298$ K the measured interfacial tension is 1.47×10^{-3} N/m. Alternatively, we can use the data obtained by Kahlweit *et al.*⁽³²⁾ for octane and decane and interpolate linearly between them, which leads to practically the same value 1.45×10^{-3} N/m. In order to compare this to the dimensionless quantity γ_{MA} of the theory we need to multiply this with the area of a unit cell in the lattice model, since the distance z is in these units, and to divide by $k_B T_c$, with $T_c = 352$ K.

The lattice constant σ is the representative nearest-neighbour distance of a molecular pair. In the lattice model σ is in principle determined through the number density at the consolute point, through the relation

$$(\rho_M + \rho_A) \sigma^3 = 1, \quad (3.11)$$

where $\rho_{M(A)}$ is the number of methanol (alkane) molecules per unit volume. While this relation is, strictly speaking, reserved for $T = T_c$, it is actually imposed for all T in the lattice approximation, since all the cells are filled either by a M or an A particle. The σ defined in this way lies in between the molecular diameters of the two components, σ_M and σ_A , as we will illustrate for methanol and nonane in Section 5. In what follows we adopt a simple approximation and just take the arithmetic mean, $\sigma = (\sigma_M + \sigma_A)/2$.

For methanol $\sigma_M \approx 3.65$ Å (valid for both Lennard-Jones and Stockmayer potentials), while for nonane we may deduce an effective

diameter $\sigma_A \approx 5.99 \text{ \AA}$ from the excluded volume or “hard-sphere” volume. We adopt this useful approximation even if the molecules are of ellipsoidal rather than spherical shape.^(28,29) The relation between the excluded volume and the associated parameter b in the van der Waals equation of state is

$$b = 2\pi\sigma^3/3, \quad \text{with} \quad b = kT_c^{\text{LG}}/8P_c^{\text{LG}}, \quad (3.12)$$

where P_c^{LG} is the critical pressure of the fluid. Note that if we use, e.g., the more complicated Peng–Robinson equation of state,⁽³³⁾ a smaller diameter $\sigma_A \approx 5.11 \text{ \AA}$ is obtained. This value is almost certainly an underestimation, because it leads to a molecular mass density of nonane that is higher than that of methanol, in contradiction with the experimental fact that the methanol-rich phase is heavier than the nonane-rich phase.

For the van der Waals equation of state we conclude $\sigma \approx 4.83 \text{ \AA}$, by taking the arithmetic average. The result for the dimensionless interfacial tension is $\gamma_{MA} = 0.0706$, using experimental data,⁽³¹⁾ and $\gamma_{MA} = 0.0696$, interpolating between experimental data.⁽³²⁾ This leads to $c = 0.587$ and $c = 0.579$, and hence $K_c = 0.173$ and $K_c = 0.171$, respectively. This is an interesting result, close to the values appropriate to the lattices we considered, and very close to the mean-field value $1/6$ for the SC lattice. Alternatively, for the Peng–Robinson equation of state the results are $K_c = 0.117$ and $K_c = 0.113$, respectively, which is close to the mean-field value for the BCC lattice. While being aware of the quantitative sensitivity of these results to the choice of equation of state, we expect to obtain a qualitatively correct description by using the σ obtained from the simplest one (van der Waals).

We now turn to the identification of the surface field h_1 and the surface coupling enhancement g in the surface free-energy functional. For the surface field we have the simple relation,⁽²⁶⁾

$$h_1 = H_{\text{surf}}/k_B T_c \quad (3.13)$$

where T_c is the consolute-point temperature. For the enhancement we have, for $T/T_c \approx 1$,

$$g = -mK_c \quad (3.14)$$

with $m = 1$ for the SC lattice,⁽²⁶⁾ and $m = 4$ for the FCC lattice. We conclude that, since $g < 0$, first-order as well as critical wetting transitions are possible, in principle, as was first demonstrated by Nakanishi and Fisher,⁽²²⁾ who derived the global wetting phase diagrams within Cahn–Landau theory.

4. CROSSOVER FROM FIRST-ORDER TO CRITICAL WETTING: SHORT-RANGE FORCES

The Cahn–Landau theory developed so far does not include the effects of the “tails” of the intermolecular van der Waals forces, but only takes into account the short-range part of these forces. Such short-range forces can be constructed artificially, for example, when the tails of the pair potentials are “cut off” at, e.g., radial distance 2.5σ as is often done in Molecular Dynamics simulations of fluids.⁽³⁴⁾ Our first concern is to check, within the short-range forces frame-work, the order of the wetting transition predicted for the *n*-alkane/methanol mixtures. To this end we make use of the results derived in ref. 30. However, the notation of that paper cannot be applied directly, because the definitions of the bulk free energy densities f differ by a factor 12 between that work and the present one (which uses the definitions of ref. 26). If we take this into account we find that *tricritical wetting* occurs for

$$\kappa \equiv \sqrt{12} g/c\phi_0 = -2 \quad (4.1)$$

Critical wetting takes place for $\kappa < -2$ and first-order wetting results for $\kappa > -2$ (which includes also $g > 0$).

For wetting or drying transitions close to T_c we can use the previously mentioned expression (3.14) for g . If the transition is not very close to T_c we can use the more general result,⁽²⁶⁾ which includes a correction of first order in $1 - T/T_c$, and replace g by $g + (1 - T/T_c)/2$. Likewise, for ϕ_0 we can use (3.5) or the more generally valid value which results from solving the equation

$$\phi_0 = \tanh(T_c\phi_0/T) \quad (4.2)$$

Using as input the experimentally determined transition temperatures, we give the results for κ , for both methods and for the two lattices concerned, in Table I.

Experimentally, the hexane/methanol mixture shows a wetting phase transition, with hexane as the wetting component, at $T_w/T_c \approx 0.92$. Since in this case the alkane-rich phase wets the liquid-vapour interface, methanol droplets detach from this interface. This can be called a “drying” transition, if we agree always to refer to methanol as the “wetting” component. This leads to $\kappa > -2$ assuming SC packing and $\kappa < -2$ for FCC, so that the theory, based on short-range forces alone, would locate this transition not far from the tricritical point, but probably still in the critical drying regime. For the heptane/methanol mixture the drying transition takes place at $T_w/T_c \approx 0.985$, leading to estimates for κ well inside the critical

Table I. Mean-Field Values for the Reduced Surface Coupling Enhancement κ , Within Cahn–Landau Theory for Short-Range Forces, Based on the Experimentally Determined Wetting Temperatures for Each Mixture^a

mixture	SC (app1)	SC (app2)	FCC (app1)	FCC (app2)
<i>n</i> -hexane/methanol	−2.04	−1.60	−5.77	−5.25
<i>n</i> -heptane/methanol	−4.72	−4.53	−13.34	−13.10
<i>n</i> -nonane/methanol	−6.10	−5.93	−17.25	−17.01
<i>n</i> -decane/methanol	−2.75	−2.43	−7.79	−7.40
<i>n</i> -undecane/methanol	−1.82	−1.33	−5.16	−4.58

^a SC (Simple Cubic) refers to a packing of molecules with coordination number 6, and FCC (Face-Centered Cubic) corresponds to dense packing with coordination number 12. App1 corresponds to the approximations (3.5) and (3.14) valid close to T_c , while app2 corresponds to using the enhancement $g+(1-T/T_c)/2$ and (4.2). First-order wetting is predicted for $\kappa > -2$ and critical wetting for $\kappa < -2$, the tricritical value being $\kappa = -2$.

drying range. For octane/methanol no transition was detected. Possibly it occurs very close to T_c . For these three systems no detailed measurements were made to study the order of the drying transition.

A clear first-order wetting transition, on the other hand, was observed for undecane/methanol, with methanol as wetting phase, at $T_w/T_c \approx 0.903$. The resulting κ -values satisfy $\kappa > -2$ (SC) and $\kappa < -2$ (FCC), which indicates that this transition is not far from the tricritical wetting point ($\kappa = -2$) if we neglect the tails of the van der Waals forces. For decane/methanol $T_w/T_c \approx 0.955$, so that all κ -estimates are already within the critical wetting range. This is more pronounced still for the nonane/methanol mixture, with $T_w/T_c = 0.992$. For this last mixture short-range critical wetting is observed experimentally. This suggests that the effect of the van der Waals forces on this transition is quite weak. The scrutiny of this is the subject of the next section.

On the basis of the results in Table I we can locate approximately the tricritical wetting point, corresponding to the choice of the SC lattice. For both approximations (first and second column of Table I) we obtain that the tricritical condition $\kappa = -2$ falls between decane and undecane. Decane/methanol is predicted to show critical wetting and undecane/methanol to display first-order wetting. More precisely for the first approximation, valid close to T_c , we obtain $T_w/T_c = 0.917$ for tricriticality. Using linear interpolation this leads to an effective chain length of 10.72, which can in principle be achieved by using mixtures.⁽³⁵⁾ For the second approximation the tricritical point is at $T_w/T_c = 0.941$ and chain length 10.27. Both of these estimates from this theory with only short-range forces are in qualitative agreement with our recent experiments which indicate a crossover

from first-order to critical wetting with a tricritical wetting point between an effective alkane carbon number of 9.6 and 10.⁽³⁵⁾ Since the results for both approximations do not differ significantly, in contrast to the results for different choices of lattices, we will henceforth adopt the simple first approximation valid close to T_c , unless stated otherwise.

In the remainder of this section we illustrate typical results based on the short-range-forces theory, and compute the layer thickness, the adsorption, and the pertinent surface free energies versus temperature, at fixed bulk field very close to two-phase coexistence. We recall that bulk coexistence corresponds to the condition $h = 0$. In view of (2.3), (2.4), and (2.9) this reads $(\mu_M - \mu_A) + q(\epsilon_{MM} - \epsilon_{AA})/2 = 0$. Since our system is in a gravitational field and the chemical potential of a particle (as defined in the absence of the field) depends on its height through a gravitational potential energy contribution, this equality is only satisfied at one particular height, which is, of course, the position of the *liquid-liquid* interface. At a small elevation L_e above this interface, where the liquid-vapour interface is situated, there is a non-zero bulk field $h < 0$, favouring alkane molecules. Since we have put all particles on a lattice with a single lattice constant, the magnitude of h depends not only on the difference in molecular weight of M and A molecules, but also on the specific volume per molecule in the real liquid mixture. In Section 5 we estimate h , give an explicit expression for it, and show that it is essentially independent of temperature. We can therefore perform all calculations at fixed $h < 0$ for all relevant T , below, at, and above T_c .

We will focus on 3 cases: first-order wetting ($\kappa = 0$, for example), tricritical wetting ($\kappa = -2$) and critical wetting ($\kappa = -10$, for example). Before embarking on these cases, we discuss some generalities concerning the order parameter and the free energy.

4.1. The Wetting Layer Thickness

When a sufficient amount of methanol is adsorbed at the alkane/vapour interface, it is convenient to define a layer thickness l , which corresponds to the region occupied by a methanol-rich film. In our model l is measured from $z = 0$ down to the position $z = l$ where the concentration almost equals that of the alkane-rich phase, which is the bulk concentration. There is some freedom in defining where precisely this bulk phase starts, and the results are not sensitive to this definition, as long as it remains reasonable. We choose to define l implicitly so that $\phi(l) = 0.9\phi_b$, which is useful even for small adsorbed amounts. For thick wetting films on the other hand, the simpler definition $\phi(l) = 0$ would work equally well. Both types of choices were examined previously when studying alkanes on

water.⁽³⁶⁾ Incidentally, note that the choice $\phi(l) = \phi_b$ is not possible, since it would result in $l = \infty$ in view of the exponential decay of the concentration to its bulk value.

4.2. The Adsorption or Coverage

The arbitrariness in the definition of the layer thickness is avoided when working with the alternative order parameter, the adsorption or coverage. This is a measure of the total adsorbed amount per unit area, obtained by integrating the concentration excess. The adsorption Γ is thus defined as

$$\Gamma = \int_0^{\infty} dz(\phi(z) - \phi_b) \quad (4.3)$$

There is a close connection between the adsorption and the experimentally measured quantity. In the particular case of binary liquid mixtures that we study, the experiment makes use of ellipsometry, and the measured ellipticity is proportional to the adsorption at the liquid-vapour interface,⁽³⁷⁾ provided the wetting layer thickness does not exceed 1000 Å. This condition is well satisfied in all our experiments. Working with the adsorption is all the more useful since in the thin-film regime experiments have been performed with only a small amount of excess material adsorbed at the interface and in this case a layer thickness is hard to define.

4.3. The Surface Free Energies

If the measurements were performed precisely at two-phase coexistence of the methanol-rich and alkane-rich phases, one could work with the three interfacial tensions γ_{VA} , γ_{VM} and γ_{MA} , which are defined as follows. The interfacial tension between methanol and alkane has already been defined in (3.10), and is an absolute quantity, since no unknown constant intervenes. The interfacial tension γ_{VA} between the vapour and the alkane-rich phase can be calculated by minimizing (3.7) with the bulk condition $\phi \rightarrow \phi_b < 0$, and likewise γ_{VM} is obtained using the bulk condition associated with the methanol-rich phase, $\phi_b > 0$. The latter two surface free energies are relative quantities, which can be seen most easily from the fact that it follows from the theory that they are zero at the bulk consolute point, for a spatially constant order parameter $\phi(z) = 0$. The true interfacial tension for that hypothetical profile is a constant, γ_0 , the value of which we do not need to know.

We now define the *equilibrium spreading coefficient* S ,

$$S = \gamma_{VA} - (\gamma_{VM} + \gamma_{MA}) \quad (4.4)$$

Partial wetting corresponds to $S < 0$. In this case Young's law allows us to obtain the contact angle θ which a methanol-rich droplet makes against the alkane/vapour interface,

$$\gamma_{VA} = \gamma_{VM} + \gamma_{MA} \cos \theta \quad (4.5)$$

Complete wetting corresponds to an equilibrium spreading coefficient equal to zero, but if we denote by γ_{VA}^* the free energy of a *stable or metastable* surface state with a thin adsorbed film of the methanol-rich phase, then we can define within mean-field theory a more general *spreading coefficient* S^* through

$$S^* = \gamma_{VA}^* - (\gamma_{VM} + \gamma_{MA}) \quad (4.6)$$

With this definition, $S^* > 0$ for the complete wetting regime between the wetting transition and the upper spinodal point. S^* ceases to be defined for temperatures above this spinodal, as γ_{VA}^* is no longer defined.

A first-order wetting transition is then characterized by a simple zero-crossing of S^* . Critical wetting is more subtle, because in this case there is no metastable extension of the thin film. S approaches zero from below, with vanishing slope, without crossing zero. In this case, a generalization S^* different from S does not exist.

Due to gravitational effects the methanol-rich phase is slightly off of coexistence, while the alkane-rich phase is stable in bulk, at the elevation at which the alkane/vapour interface and the methanol wetting layer reside. Typically, this elevation is 5 mm above the methanol/alkane interface. In practice, while we can calculate under these circumstances the quantity γ_{VA} , we must have recourse to approximations for computing the other two surface free energies. We will address this interesting problem for the cases of first-order and critical wetting separately.

Case 1. First-Order Wetting

When the wetting transition is of first order, we can, for our present purpose of illustrating the method, restrict our attention to zero surface coupling enhancement, $g = 0$. Then the surface field h_1 which induces the transition is given by the relation⁽³⁰⁾

$$h_1 = 0.681 c \phi_{0,w}^2 / \sqrt{12}, \quad (4.7)$$

where $\phi_{0,w}$ denotes the value of ϕ_0 and therefore the temperature at which the wetting transition takes place. We take $\phi_{0,w} = 0.2$ so that $T_w/T_c = 0.987$. The factor $\sqrt{12}$ is present because our units are different from those of ref. 30. Of special interest for us is also the upper spinodal, corresponding to the metastability limit of the thin film upon increasing the temperature towards T_c . This point is located at

$$\phi_{0,sp}^2 = \sqrt{12} h_1 / c, \quad (4.8)$$

where h_1 is the surface field defined in (4.7) and $\phi_{0,sp}$ determines the spinodal temperature. In the experiments the wetting layers occur at a height where the wetting phase is slightly undersaturated, corresponding to $h \approx -10^{-6}$ (see Section 5). Here we take a somewhat larger undersaturation, $h = -10^{-5}$, for greater clarity of presentation. We will encounter the prewetting transition and the upper prewetting spinodal at slightly higher temperatures than the wetting transition and associated spinodal at bulk coexistence. As was mentioned already, the undersaturation (in methanol) is a consequence of the gravitational contribution to the chemical potential. The main effect of this is that the wetting layer cannot reach macroscopic thickness. For a more detailed study of first-order wetting transitions under gravity, we refer to reference.⁽³⁸⁾ On the other hand the lower prewetting spinodal, which is the metastability limit of the thick film upon decreasing the temperature, typically lies at a temperature far below that of the equilibrium phase transition.⁽³⁹⁾

The phase portrait follows from the first integral or “constant of the motion” derived from the Euler–Lagrange equation⁽³⁰⁾

$$\frac{c^2}{2} \frac{d^2\phi}{dz^2} = \frac{df}{d\phi} \quad (4.9)$$

This conservation law reads, with $\dot{\phi} \equiv d\phi/dz$,

$$\dot{\phi} = \pm 2 \sqrt{f(\phi)} / c \quad (4.10)$$

While we will work with the SC microscopic lattice model in the applications to the experiments (Section 5), in this methodological section we work, for a change, with the FCC lattice. We therefore have $c^2/2 = K_c = 1/12$ in MF theory, implying $c = 1/\sqrt{6}$. With this choice the value of h_1 is fixed by (4.7) and equals 0.00321. The bulk condition reads

$$\phi(z) \rightarrow \phi_b, \quad \text{for } z \rightarrow \infty \quad (4.11)$$

which corresponds to the alkane-rich phase. The boundary condition at the liquid-vapour interface⁽³⁰⁾ reads

$$\dot{\phi}|_{z=0} = -2h_1/c^2 \quad (4.12)$$

Figure 1 shows the thickness l of the thin film and the thick film as a function of temperature, for fixed h_1 and $g = 0$. The calculations have been performed for temperatures below as well as above the consolute temperature T_c . For $T > T_c$ there is no wetting layer, since the bulk phases are fully mixed into a single phase. However, the preferential adsorption of methanol at the liquid/vapour interface remains visible as a methanol-enriched transition zone, which close to T_c is called *critical adsorption*.

We distinguish the thin film and the wetting layer, which, strictly speaking, is a prewetting layer. The wetting transition (more precisely, prewetting transition), where the film and the layer exchange stability, is indicated by the vertical dashed line. The thin film is stable at low temperature, becomes metastable above the wetting point and remains metastable up till the spinodal temperature (open circle). The wetting layer is metastable below the wetting point and stable above it. When the temperature

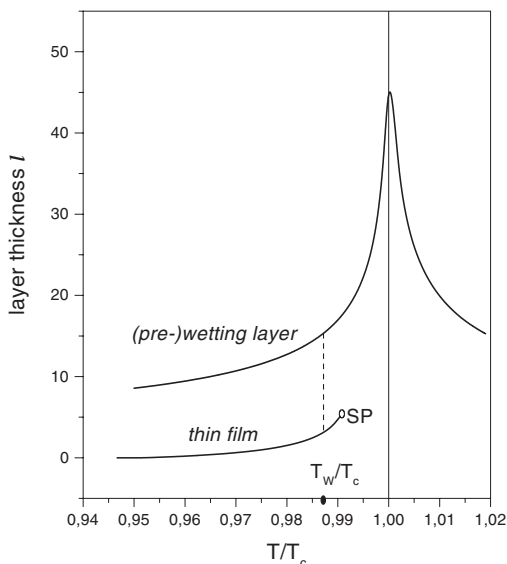


Fig. 1. Layer thickness versus temperature for the case of a first-order (pre-)wetting transition at $T_w/T_c = 0.987$ (dashed line) in the model with short-range forces. The spinodal point (SP) marks the metastability limit of the thin film. The wetting layer thickness displays a sharp maximum at the bulk consolute point, $T = T_c$.

crosses T_c the wetting layer state gradually changes to a state in which a methanol-rich layer sits on a single (fully mixed) bulk phase.

Close to the critical point there is a marked increase in the layer thickness, below as well as above T_c . This is related to the well-documented phenomenon of critical adsorption,⁽⁴⁰⁾ which entails a slow (algebraic) decay of the concentration profile into the bulk phase in place of the usual exponential decay, in this theory, governed by the length scale set by the bulk correlation length ξ . The divergence of ξ at T_c leads to a diverging layer thickness, as we have defined it. Since this effect is sensitive to the definition of the layer thickness, it is preferable to study the adsorption Γ , to which we now turn.

Figure 2 shows how the adsorption Γ varies with temperature, for the case of first-order wetting. The vertical line denotes the wetting transition as in Fig. 1. In contrast with the layer thickness, the adsorption gives a unique and reliable estimate of the concentration excess near the liquid/vapour interface. In the thin-film state the adsorption follows closely the layer thickness variation. However, in the wetting layer the adsorption

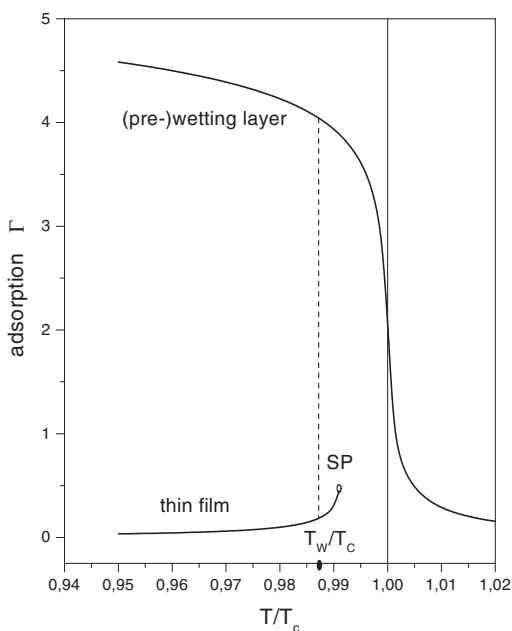


Fig. 2. Adsorption versus temperature for the case of a first-order (pre-)wetting transition (dashed line) in the model with short-range forces. The spinodal point (SP) marks the metastability limit of the thin film. The phenomenon of critical adsorption is clearly visible when the temperature is lowered from near-critical values above T_c , through T_c .

behaves qualitatively differently from l . Well below T_c the adsorption depends on the undersaturation, described by the bulk field h . If h is decreased to zero, the wetting layer becomes macroscopically thick and the adsorption diverges. In mean-field theory this divergence is logarithmic in $1/|h|$, as our computations confirm. On the other hand, close to and at T_c the adsorption varies rapidly as a function of temperature (at fixed undersaturation), as Fig. 2 shows. The value of Γ at T_c , as a function of h , is described by the scaling laws of critical adsorption.⁽⁴⁰⁾ In mean-field theory there is (again) a logarithmic divergence in $1/|h|$, while for real fluids the divergence is of the power-law form

$$\Gamma \propto |h|^{(\beta-\nu)/\Delta} \quad (4.13)$$

where $\beta \approx 0.33$ and $\nu \approx 0.63$ are the bulk order-parameter and correlation-length exponents, respectively, and $\Delta \approx 1.56$ is the bulk gap exponent which appears when temperature-like exponents are converted to field-like ones. In mean-field theory $\beta = \nu = 1/2$ and $\Delta = 1.5$.

The combined result of the increased adsorption at T_c and the presence of the wetting layer below T_c is what is seen in Fig. 2. We would like to stress that the monotonic behaviour of $\Gamma(T)$ displayed here is not the only possible one. Depending on the undersaturation, which opposes wetting, and the precise magnitude of the surface field favouring wetting, non-monotonic adsorption and critical depletion phenomena can also occur,⁽⁴¹⁾ when the temperature approaches T_c from above.

Turning now to the surface free energy, Fig. 3 shows this quantity for the thin film and for the wetting layer. The first-order character of the wetting transition is clearly seen from the crossing of the free energy branches, and the upper spinodal is also indicated. Due to the slight undersaturation a spreading coefficient cannot be defined rigorously, but for small $|h|$ a very good approximation to S^* defined in (4.6) is given by

$$S^* \approx \gamma_{\text{thin}} - \gamma_{\text{thick}} \quad (4.14)$$

Clearly, $S^* < 0$ for the thin film, and $S^* > 0$ for the wetting layer. In reality, S^* is slightly larger than this approximation by an amount of the order of $-h(l_{\text{thick}} - l_{\text{thin}})$, where l is the layer thickness. For small h , as for our calculations, this correction is unimportant.

Case 2. Tricritical Wetting

The tricritical wetting transition takes place for the following special values of the surface coupling enhancement g and surface field h_1 ,⁽³⁰⁾

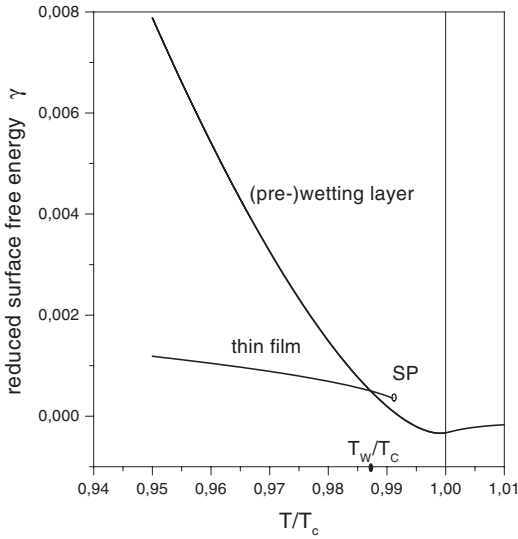


Fig. 3. The excess surface free energy per unit area relative to some unknown common constant, for the thin film and the wetting layer. The crossing point of the curves indicates the discontinuous (first-order) (pre-)wetting transition for the model with short-range forces.

$$g = -2 c \phi_{0,w} / \sqrt{12} , \tag{4.15}$$

$$h_1 = -g \phi_{0,w} \tag{4.16}$$

Again we fix the wetting transition at $\phi_{0,w} = 0.2$ so that $T_w/T_c = 0.987$ and we use the same lattice parameters (FCC) as in the previous case. The computation of the layer thickness l is straightforward and for a bulk field $h = -10^{-6}$, in the experimentally relevant range, the result is shown in Fig. 4 (curve “tcw”). The most remarkable feature of this figure is the weakness of the layer thickness increase in the vicinity of the wetting transition, at $T/T_c \approx 0.987$. In order to see a stronger increase of l , the bulk field must be made smaller in magnitude than the 10^{-6} we have chosen. However, a smaller value of $|h|$ will also lead to a larger value of l at T_c , associated with the diverging bulk correlation length at bulk criticality. With our choice of h we have attempted to visualize the two effects using the same scale of l . The value of l at T_c is $l_c = 106.3$.

For comparison with experimentally measured quantities, it is more appropriate to study the adsorption Γ . The result of the calculation for the same field $h = -10^{-6}$ is shown in Fig. 5 (curve “tcw”). Now the tricritical

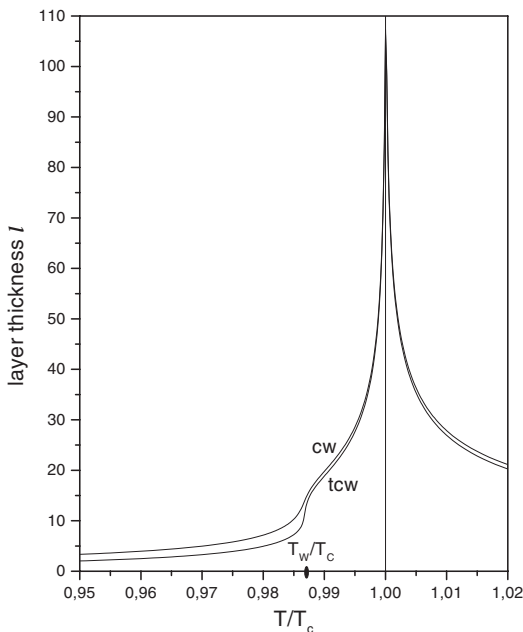


Fig. 4. Layer thickness versus temperature, slightly off of bulk coexistence, in the vicinity of a tricritical wetting transition (tcw) and a critical wetting transition (cw) in the model with short-range forces, occurring at $T_w/T_c = 0.987$. The (pre-)wetting layer thickness displays a sharp maximum at the bulk consolute point, $T = T_c$. Note how weak the wetting signal is compared to the peak at bulk criticality, with this choice of order parameter l .

wetting transition at $T_w/T_c \approx 0.987$ is clearly detectable as well as the critical adsorption phenomenon for T/T_c approaching 1. This is how, in the theory dealing with short-range forces alone, both phenomena manifest themselves when the adsorbate is slightly off of two-phase coexistence in bulk (by fixing h). Comparing this with the adsorption calculated for a first-order wetting transition (and somewhat larger bulk field magnitude), shown in Fig. 2, we can easily distinguish the continuous and reversible adsorption at tricritical wetting from the discontinuous and hysteretic behaviour of Γ at first-order wetting.

In the experiments it is possible to measure contact angles, and therefore the spreading coefficient, in spite of the slight undersaturation of the wetting phase at the liquid-vapour interface. It would thus be very welcome to be able to calculate θ or S for states slightly off of two-phase coexistence, although these quantities are, strictly speaking, not well defined under these circumstances. For the case of a first-order wetting transition

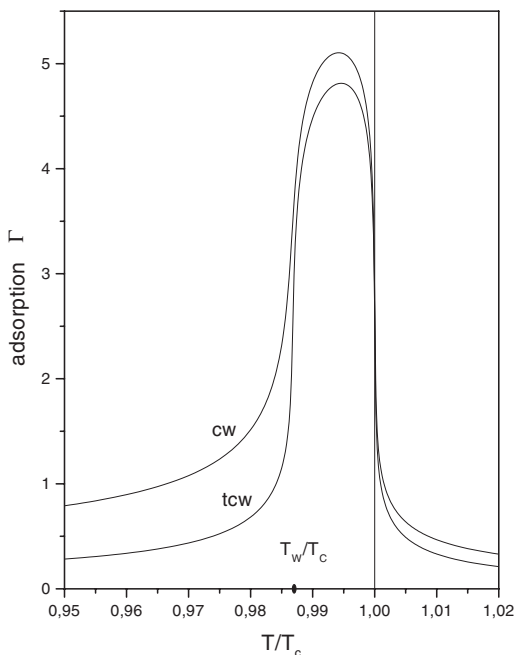


Fig. 5. Adsorption versus temperature, slightly away from bulk two-phase coexistence, in the vicinity of a tricritical (tcw) and critical (cw) wetting transition in the model with short-range forces. The wetting signals at $T_w/T_c \approx 0.987$ are comparable in strength to the critical adsorption phenomena at $T = T_c$. Note how steep is the wetting singularity for the case of tricritical wetting.

we could circumvent this problem by taking advantage of the existence of two states, the thin film and the wetting layer, so that S could be approximated as in (4.14). In the vicinity of continuous wetting transitions, however, there is only one film state, and we must have recourse to a new, more general method. In the following we develop an approximation, which allows us to calculate S for situations in which the wetting phase is metastable, but sufficiently long-lived.

For states off of coexistence, only one of the three surface tensions that feature in the spreading coefficient is well defined. In our system this is γ_{VA} , since the alkane-rich phase is stable in bulk at the height of the liquid-vapour interface, while the methanol-rich phase is metastable. We denote this metastable phase by M^* . In Fig. 6 we have sketched the configuration of a metastable droplet of methanol attached to the alkane-vapour interface, for which we would like to calculate S and hence obtain

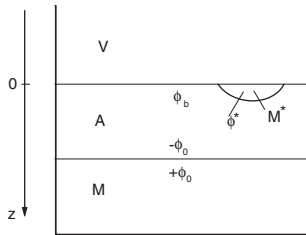


Fig. 6. The configuration of our system with vapour (V), alkane-rich (A) and methanol-rich phases (M), showing the metastable droplet of the methanol-rich phase, M^* , attached to the alkane-vapour interface at height $z = 0$. Not shown is the (microscopic) thin film of M at the A-V interface. Bulk two-phase coexistence is achieved at the A-M interface, but not at the A-V interface, where slight gravitational undersaturation of the A phase in the M component takes place. The bulk concentration at $z = 0$ is indicated by ϕ_b and differs slightly from the coexistence value $-\phi_0$.

the contact angle from the Young equation. We begin by formally defining the following approximation to S ,

$$S \approx \gamma_{VA} - (\gamma_{VM^*} + \gamma_{M^*A}) \quad (4.17)$$

Our task is now to give meaning to and to calculate the last two terms.

In spite of its thermodynamic metastability the attached droplet is in mechanical equilibrium, and it takes a long time (typically weeks) before the droplet disappears, through diffusion, and its content eventually joins the methanol-rich phase at the bottom. Clearly, all three interfacial tensions are measurable and should therefore be calculable, in principle. Their calculation is most easily explained by examining the phase portrait^(27, 36) shown in Fig. 7. The solid lines with arrows give the trajectories, which start at points that obey the boundary condition

$$\dot{\phi}|_{z=0} = -2(h_1 + g\phi_1)/c^2 \quad (4.18)$$

and which end at the bulk fixed point, at ϕ_b , or at the metastable bulk fixed point at ϕ^* . The trajectory from ϕ_1 to ϕ_b is the one that minimizes γ_{VA} .

We propose to define γ_{VM^*} as the excess surface free energy relative to the metastable bulk phase M^* . This excess quantity is defined using the modified functional

$$\gamma^*[\phi] = \int_0^\infty dz \left\{ \frac{c^2}{4} \left(\frac{d\phi}{dz} \right)^2 + f^*(\phi(z)) \right\} - h_1\phi_1 - g \frac{\phi_1^2}{2}, \quad (4.19)$$

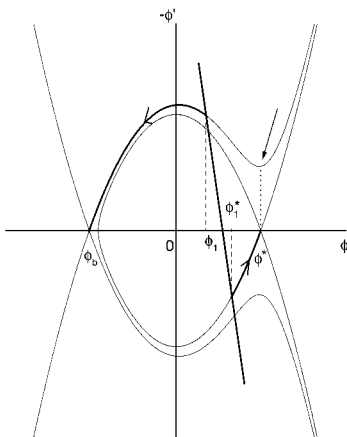


Fig. 7. Phase portrait construction allowing, approximately, to calculate the interfacial tension between the vapour V and metastable M^* phases, and between the latter and the stable A phase. The thick straight line represents the boundary condition. The dashed lines mark the surface values of ϕ at the V-A or V- M^* interfaces. The thick curves give the trajectories of these two interfaces. The dotted line and the accompanying arrow indicate, respectively, the jump in the derivative of ϕ at the M^* -A interface, and the starting point of the trajectory which, from this interface, eventually leads to the bulk A phase. For this figure the value $h = -0.0001$ was used for the bulk field.

where $f^*(\phi)$ is the bulk free energy density *relative to the metastable state*,

$$f^*(\phi) = -h(\phi - \phi^*) - (1 - T/T_c)(\phi^2 - \phi^{*2})/2 + (\phi^4 - \phi^{*4})/12 \quad (4.20)$$

Minimization of this functional gives the trajectory which runs from ϕ_1^* to ϕ^* .

Finally, we define the interfacial tension between the metastable and stable bulk phases M^* and A as follows. Since the alkane-rich phase is stable in bulk, it is obvious that we must define γ_{M^*A} as the excess free energy relative to the stable phase, and therefore use $f(\phi)$ defined in (3.6). Furthermore, the trajectory must start at ϕ^* and end at ϕ_b . The optimal concentration profile, which minimizes the surface free energy, does not start with zero derivative, but with a finite value of $\dot{\phi}$ (see dotted line in Fig. 7). This small jump in derivative is caused by the slight undersaturation of the metastable phase, and vanishes for $h \rightarrow 0$. In that limit γ_{M^*A} approaches γ_{MA} given by (3.10).

The approximation scheme we adopt neglects the excess free energy in bulk of M^* relative to A in calculating γ_{VM^*} , since we use f^* in place of f . This contribution is to be multiplied with the thickness, along z , of the

region occupied by the M^* phase, in order to obtain the excess surface free energy. Hence, our approach, which is an approximation assuming small undersaturation, should be more accurate for small droplets than for large ones. Note that for small undersaturation droplets of a wide range of sizes can be observed as being metastable.

The result of the approximation is shown in Fig. 8. The two surface free energy curves approach one another almost tangentially, at $T/T_c \approx 0.987$. At this point the curves actually cross. However, this cannot be seen on the scale of the figure. The curves appear coincident for $T/T_c > 0.987$. For example, at $T/T_c = 0.99$ the difference in reduced surface free energy is only about 2×10^{-6} . The crossing of the curves is due to the fact that the system is slightly off of coexistence. In the limit $h \rightarrow 0$ the curves meet tangentially at the tricritical wetting point, and the curve associated with γ_{VA} stops there. This is in contrast with Fig. 3, where the thin-film state

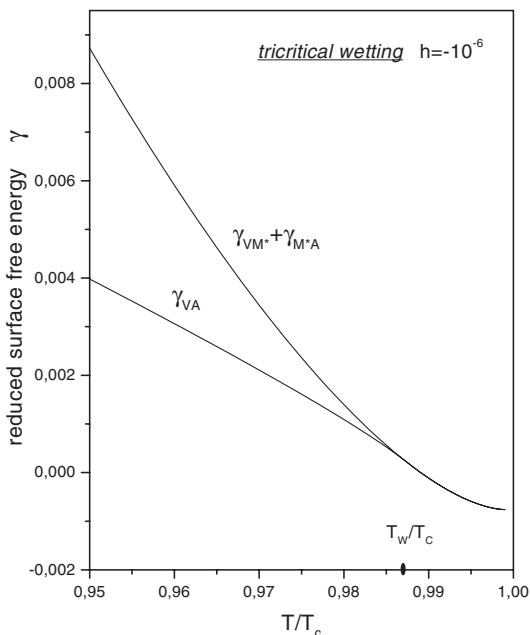


Fig. 8. Dimensionless surface free energy versus temperature for a system with short-range forces in the vicinity of a tricritical wetting transition. The lower curve is for the V-A interface and the upper one is for the combination of the V-metastable M and metastable M-A interfaces, computed with the new approximation scheme. Due to the presence of a very small but nonzero bulk field h the curves approach each other tangentially and actually cross at the approximate tricritical wetting point at $T_w/T_c \approx 0.987$. On the scale of the figure the curves appear to merge.

continues to exist as a metastable state up till the spinodal point. In fact, tricriticality is achieved when the spinodal coincides with the wetting transition itself. The difference of the two curves of Fig. 8 gives the spreading coefficient, which will be discussed together with that for critical wetting.

Case 3. Critical Wetting

The critical wetting transition takes place under the following restrictions of the surface coupling enhancement g and surface field h_1 ,⁽³⁰⁾

$$g < -2 c\phi_{0,w}/\sqrt{12}, \quad (4.21)$$

$$h_1 = -g\phi_{0,w} \quad (4.22)$$

In this range we choose $g = -10 c\phi_{0,w}/\sqrt{12}$, and the wetting temperature, bulk field and lattice parameter are chosen the same as for the previous case of tricritical wetting. The result for the layer thickness l is shown in Fig. 4 (curve "cw"). As in the previous case, the increase of l in the vicinity of the critical wetting transition at $T_w/T_c \approx 0.987$ is quite weak compared with the critical adsorption peak at T_c . The value of l at T_c equals $l_c = 107.3$. Further, the critical wetting transition presents a weaker signal than the tricritical wetting transition.

The comparison between tricritical and critical wetting can be made most clearly in Fig. 5, which shows the adsorption. The behaviour at critical wetting is continuous, while the tricritical transition is almost discontinuous, which is to be expected in view of the fact that tricriticality marks the onset of the regime of first-order (discontinuous) transitions.

The calculation of the surface free energy proceeds along the approximation scheme outlined in the previous section, and the result is shown in Fig. 9. As in the case of tricritical wetting, the two curves approach each other almost tangentially at the wetting point. The difference of the two curves determines the spreading coefficient S , which is shown in Fig. 10 for the three cases: critical wetting (cw), tricritical wetting (tcw), and first-order wetting (fow). For this comparison, the same bulk field, $h = -10^{-6}$, was imposed. As expected, S crosses zero linearly for first-order wetting, while S approaches zero with vanishing slope for the continuous wetting transitions.

The singular behaviour of S at wetting is described by the power law, for T approaching T_w from below,

$$S = S_0(T_w - T)^{2-\alpha_s} \quad (4.23)$$

where α_s is the surface specific heat exponent. At bulk two-phase coexistence ($h = 0$) the Cahn–Landau theory produces the mean-field results for

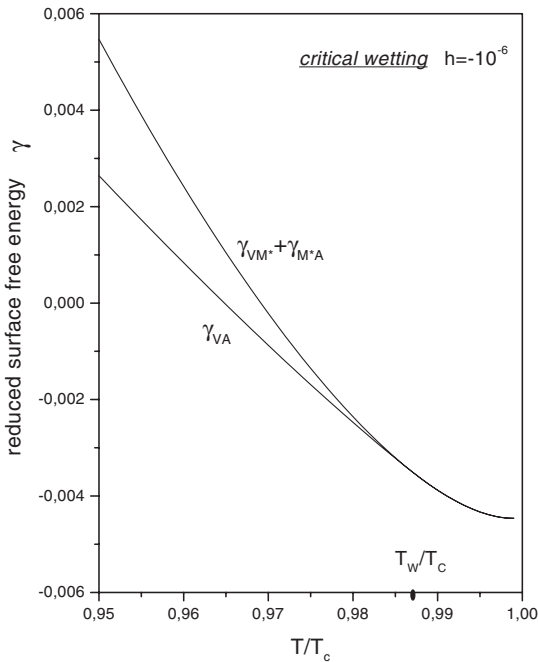


Fig. 9. Dimensionless surface free energy versus temperature for a system with short-range forces in the vicinity of a critical wetting transition. The lower curve is for the V-A interface and the upper one is for the combination of the V-metastable M and metastable M-A interfaces, computed with the new approximation scheme. Due to the presence of a very small but nonzero bulk field h the curves approach each other tangentially and actually cross at the approximate critical wetting point at $T_w/T_c \approx 0.987$. On the scale of the figure the curves appear to merge.

short-range forces, $\alpha_s = 1$ (fow), $\alpha_s = 1/2$ (tcw), and $\alpha_s = 0$ (cw). Since our spreading coefficients are extensions of S away from two-phase coexistence, a condition relevant to the experimental situation, it is instructive to check whether these asymptotic exponents already show up sufficiently clearly. For “fow” there is a zero-crossing, so that S is linear about T_w , implying $\alpha_s = 1$. For “tcw” fits to the calculated curve give $\alpha_s = 0.40 \pm 0.10$ and for “cw” we find $\alpha_s = 0.02 \pm 0.04$, where the error bars reflect how much the results typically vary when various temperature ranges of input data are used. In conclusion, the tricritical and critical wetting transitions at $h = 0$ are already well approximated by the behaviour of S slightly off of coexistence. This is valid for systems with short-range forces. In order to compare the theory with experiments on real fluids, however, it is indispensable to include the long-range forces in the description, which is the task to which we now turn.

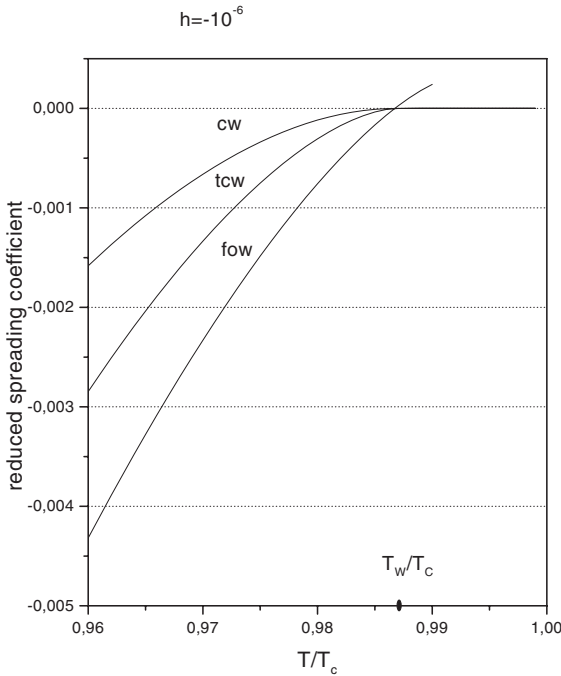


Fig. 10. Dimensionless spreading coefficients S for first-order wetting (fow), tricritical wetting (tcw) and critical wetting (cw), for systems slightly removed from bulk coexistence by a small bulk field $h = -10^{-6}$ and for short-range forces. For first-order wetting S clearly displays a zero-crossing at the transition, implying $2 - \alpha_s = 1$. For the continuous transitions S vanishes with vanishing slope, to a very good approximation, so that $\alpha_s < 1$. For tricritical wetting $\alpha_s \approx 1/2$ and for critical wetting $\alpha_s \approx 0$. Precise values are given in the text.

5. CROSSOVER FROM FIRST-ORDER TO CRITICAL WETTING: LONG-RANGE FORCES

In this section we include the long-range tails of the van der Waals interactions between molecules in the Cahn–Landau description. In doing so we follow ref. 36 and limit ourselves to allowing for a long-range substrate-adsorbate field $h(z)$ which takes into account the net effect of the substrate-adsorbate adhesive and adsorbate-adsorbate cohesive contributions which influence the thickness of the wetting film. The extended Cahn–Landau free-energy functional reads

$$\gamma[\phi] = \int_0^\infty dz \left\{ \frac{c^2}{4} \left(\frac{d\phi}{dz} \right)^2 + f(\phi(z)) \right\} - \int_{z^*}^\infty dz h(z) \phi(z) - h_1 \phi_1 - g \frac{\phi_1^2}{2} \quad (5.1)$$

For non-retarded van der Waals forces, relevant to wetting film thicknesses not exceeding a few hundred Å, the decay of $h(z)$ is algebraic and of the form

$$h(z) = a_3/z^3 + \mathcal{O}(1/z^4) \quad (5.2)$$

Since in our type of system the long-range interactions favour wetting by the methanol-rich phase,⁽⁴²⁾ we have $a_3 > 0$, which is referred to as “agonistic” long-range forces (LRF).⁽⁴⁾ The leading amplitude a_3 , to which we will henceforth refer as LRF amplitude can be related to the Hamaker constant, which is proportional to the leading term in the long-range interaction free energy per unit area between the interfaces that bound the wetting layer. This free energy or *interface potential* $V(l)$, for large wetting layer thickness l , is given by

$$V(l) - V(\infty) \approx 2\phi_0 \int_l^\infty dz h(z) \quad (5.3)$$

Clearly this potential implies a repulsive force for $a_3 > 0$. This force per unit area, or disjoining pressure between the two interfaces, is

$$\Pi(l) \equiv -dV(l)/dl \approx 2\phi_0 a_3/l^3 \quad (5.4)$$

In the model we will neglect all higher-order contributions to $h(z)$. This is meaningful when a_3 has no significant temperature dependence, but would not be sufficient for systems in which the Hamaker constant changes sign, necessitating the inclusion of at least two terms in $h(z)$ for describing long-range critical wetting.^(36, 13)

The long-range field is “switched on” starting at a cut-off distance z^* . Previous work has devoted special attention to the possibility of optimizing this parameter,⁽³⁶⁾ but we will adopt the simplest possible criterion and fix z^* to 2.5σ , which is the standard cut-off used in many works.

The basic characteristic of our approach is to take the LRF amplitude a_3 to be an *adjustable parameter*, since we ignore all higher-order terms. If we would consider keeping the full $h(z)$ we could determine a_3 by matching it to the Hamaker constant determined on the basis of experimental data. In spite of the existence of a theoretical framework for calculating a_3 and higher-order terms,^(24, 12, 43) we do not embark on this here in view of the sensitivity of these terms to small changes in molecular parameters and other microscopic quantities. In particular, the amplitude a_4 , i.e., the coefficient of z^{-4} in (5.2), depends on the details of the spatial variation of the particle density profiles in the liquid-vapour interface. Therefore, our LRF amplitude a_3 is taken to be an effective constant, whose magnitude is

unknown, but we assume that its sign is consistent with that of the Hamaker constant in order to capture at least qualitatively the correct asymptotics for large z . Since a quantitative determination of $h(z)$ is beyond our scope, our approach is most meaningful in the sense of a *perturbative* one, in which the LRF are treated as a weak contribution. Our purpose will thus be to test the influence of weak agonistic LRF on critical wetting and the cross-over to first-order wetting, in systems which are slightly away from bulk coexistence.

In order to get a feeling for “weak LRF” and the associated order of magnitude of a_3 , it is necessary to check the value of a_3 which follows from the Hamaker constant pertaining to the experiments. Calculation of this quantity is performed using the dielectric constants and refractive indices for all phases involved.^(28, 44) For the nonane/methanol system, for example, this leads to the function

$$\tilde{\Pi}(L) \approx A(T)/L^3 = a(T) k_B T_c / (l^3 \sigma^3) = \Pi(l) k_B T_c / \sigma^3, \quad (5.5)$$

where $A(T)$ is an energy, and L is the wetting layer thickness in Å. Since A is proportional to the (bulk coexistence) order parameter ϕ_0 , it approaches zero for $T \rightarrow T_c$. At $T_w/T_c = 0.992$, with $T_c = 352$ K, the value $A(T_w)/k_B \approx 3.5$ K is obtained, so that $a(T_w) \approx 0.010$. In order to extract a_3 we need to calculate also ϕ_0 . This can be done using (4.2) at T_w which leads to $\phi_0 = 0.164$. We thus obtain $a_3 = a/2\phi_0 \approx 0.030$. We remark that a_3 can be considered to be a constant, independent of T . In the following the LRF amplitudes for our calculations will be denoted by “weak” provided they are small compared to this estimate.

The remainder of this section is structured as follows. For the three different mixtures we estimate the bulk and surface fields, the surface coupling enhancement and calculate the adsorption as a function of temperature. We interpret the results on the basis of the knowledge of the properties of the short-range theory (especially the order and location in temperature of the wetting transition) and the effect of adding weak long-range forces. We also compute the specific heat exponent when appropriate. Adsorption curves and critical exponents are compared with the experimental results.

5.1. Nonane/Methanol

The bulk field for this system, which reflects the difference between the gravitational potential energy at the liquid-vapour interface and that at the liquid-liquid interface can be obtained as follows. Equating the free-energy-density difference between the two bulk phases, due to the presence of

a small bulk field, to the gravitational potential energy difference per unit volume we obtain the relation

$$2h\phi_0 k_B T_c / \sigma^3 = -\Delta\rho_{\text{mass}} g_m L_e, \quad (5.6)$$

where g_m is the gravitational acceleration and L_e the vertical distance between the two interfaces, which is roughly 0.5 cm in the experiments. The mass density ρ_{mass} in a given phase involves the molecular weights m of the pure components and the number densities ρ in the manner

$$\rho_{\text{mass}} = m_M \rho_M + m_A \rho_A, \quad (5.7)$$

where $m_M = 32.04$ amu and for nonane $m_A = 128.25$ amu (1 amu = 1.66×10^{-24} g). The mass density difference $\Delta\rho_{\text{mass}}$, defined as the mass density of the methanol-rich phase minus that of the alkane-rich phase, is positive.

Our first concern is to obtain a reliable order-of-magnitude estimate of h , based on experimental data. The measured mass density difference at T_w is $\Delta\rho_{\text{mass}} = 0.0216$ g/cm³. We obtained this using the same method and apparatus as was used by Chaar *et al.*⁽³¹⁾ Taking this value together with $\phi_0 = 0.164$, calculated using (4.2), and invoking the average diameter $\sigma = 4.83$ Å we find $h = -0.873 \times 10^{-6}$. Note that this is of the same order of magnitude as the bulk field assumed in our examples in the short-range theory in the previous section. An error of 10% in our estimate of σ would modify h by about 30%. Also recall that $h < 0$, as it should be in order to stabilize the alkane-rich bulk phase at the height of the liquid-vapour interface.

In our lattice-gas approximation the mass density difference $\Delta\rho_{\text{mass}}$ can be related to the concentration difference Δx_M of one of the components, using the crude approximation (3.11) according to which the total number density is constant, and we obtain

$$\Delta\rho_{\text{mass}} \approx (m_M - m_A) \Delta x_M / \sigma^3, \quad (5.8)$$

where $\Delta x_M > 0$ is the concentration of methanol in the methanol-rich phase minus that in the alkane-rich phase.

This relation relies heavily on the approximation that a single lattice constant can be employed in the model, and should therefore not be expected to be accurate. In fact, it ignores the fact that the heavier alkane molecule occupies in reality a much bigger volume than the lighter methanol molecule, and therefore gets the sign of $\Delta\rho_{\text{mass}}$ wrong. However, let us not abandon this line of reasoning yet. Since the bulk order parameter is given by

$$\phi_0 = \Delta x_M \quad (5.9)$$

we can now simplify considerably the expression for the bulk field and obtain

$$h \approx -g_m L_e (m_M - m_A) / 2k_B T_c \quad (5.10)$$

The result is $h \approx 0.806 \times 10^{-6}$. Note that this approximation, which would be fine if the molecules were of nearly the same size, accidentally reproduces the correct order of magnitude of $|h|$. Besides this fortuitous point, the merit of this simple "molecular mass"-type of approximation is that it clearly shows that h is independent of temperature, to the extent that the height difference L_e between the interfaces is constant.

In order to correct qualitatively for the error made by using a single effective diameter for the two molecules in the lattice gas model, we can work with molecular mass densities instead of molecular masses as follows. Instead of m_M and m_A we employ effective masses which reproduce the correct molecular mass densities when put in the volume σ^3 of a unit cell in the lattice. This amounts to the approximation

$$h \approx -g_m L_e (m_M / \sigma_M^3 - m_A / \sigma_A^3) \sigma^3 / 2k_B T_c, \quad (5.11)$$

and leads to the estimate $h = -0.59 \times 10^{-7}$. Now the sign is correct but the order of magnitude is less satisfactory. Since we work with alkanes similar to nonane in what follows, and we would like to exploit the knowledge of the magnitude of h as determined from experimental input, we will adopt the admittedly heuristic approximation which consists of using simply (5.10) but with the correct sign,

$$h \approx -g_m L_e |m_M - m_A| / 2k_B T_c \quad (5.12)$$

No qualitative changes are to be expected when using, for example, (5.11) instead.

The surface field h_1 is derived using (2.4) and (2.11). Since the bulk field contribution in (2.11) is negligible the surface field is determined by the difference of the pure component potential parameters and we readily obtain the estimate $h_1 = 0.0206$.

For estimating the surface coupling enhancement g , we follow the procedure outlined at the end of Section 3 for determining K_c and then use (3.14). Using the experimental values for the liquid-liquid interfacial tension and the arithmetic mean $\sigma = 4.83 \text{ \AA}$ we found $K_c = 0.173$ and $K_c = 0.171$. Since these are close to $1/6$ we assume henceforth the simple cubic lattice for describing this mixture by a lattice model. This leads to the surface coupling enhancement $g = -K_c = -1/6$.

In order to test the sensitivity of σ with respect to alternative ways of defining it, we can use experimental data at the consolute point,⁽³¹⁾ such as mass density 0.689 g/cm^3 , concentration $x_A = 0.29$, partial mass density $m_A \rho_A = 0.62 \rho_{\text{mass}}$, and use (3.11) with the result $\sigma = 5.25 \text{ \AA}$. This is somewhat larger than the average value we have chosen to work with, but still well in between the pure component σ values.

In the short-range-forces theory the wetting tricritical point for this system with $g = -1/6$ lies at $\phi_0 = 0.5$ according to (4.1), and $h_1 = 0.083$ in view of (4.16). Since the actual surface field $h_1 = 0.0206$ is smaller the wetting transition is critical. This is confirmed by calculating the adsorption in the short-range forces limit, which leads to a curve very similar to that for c_w in Fig. 5. The short-range critical wetting transition takes place at $\phi_{0,w} = -h_1/g = 0.124$, which corresponds to $T_w/T_c = 0.995$, quite close to the experimental value of 0.992. From (4.1) we obtain $\kappa = -8.06$. This value is somewhat lower than the value -6 that is given in Table I for *n*-nonane/methanol (SC lattice). The reason for this difference is that in the present section the short-range critical wetting temperature is calculated self-consistently, whereas in the calculation underlying Table I the experimental wetting temperatures are used as input.

The influence of weak agonistic long-range forces on this system can be tested by assuming a LRF amplitude $a_3 = 0.003$, ten times smaller than the reference value we calculated in the first part of this section. The prediction from all previous theoretical works is that the short-range critical wetting transition must become a first-order wetting transition (see, e.g., refs. 4, 6, and 7). However, the calculation, represented by the adsorption curve in Fig. 11, clearly reveals a continuous transition, in every respect reminiscent of the critical wetting phenomenon (c_w) apparent in Fig. 5. Moreover, the experimentally observed adsorption curve, through ellipticity measurements, is shown in Fig. 12 and is similar to this theoretical one.

The solution to this paradox lies entirely in the fact that the system is not at bulk two-phase coexistence. At coexistence the wetting transition is definitely of first order, by virtue of the interface potential barrier between the macroscopic (“infinitely” thick) wetting layer and the thin film. However, off of coexistence the system does not display first-order wetting but features a prewetting line, which is very short in temperature as well as in bulk field, for very weak long-range forces. Under those circumstances the bulk field due to the gravitational effect is large enough to make the system sneak *underneath* the prewetting critical point, and show a continuous transition instead of a (weakly) first-order one. We will clarify this scenario in more detail for the system decane/methanol in the next subsection. Since the LRF favour wetting the wetting temperature is slightly

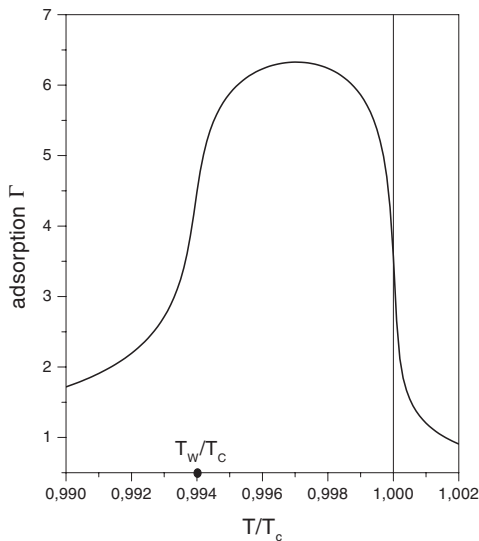


Fig. 11. Adsorption of the methanol-rich phase versus temperature for the model system representing the nonane/methanol binary liquid mixture at the liquid-vapour interface. The model parameters bulk field, surface field and surface coupling enhancement are given in the text. The amplitude of the long-range forces favouring wetting has been chosen to be very small, treating these forces as a weak perturbation. Note the continuous wetting signal at $T_w/T_c \approx 0.994$ and the critical adsorption approaching T_c from above.

lowered to $T_w/T_c = 0.994$ with respect to the short-range forces limit. Experimentally, $T_w/T_c = 0.992$ for this system.

We stress that, since we have assumed an arbitrary small a_3 , we cannot hope to obtain quantitative agreement with the experiments. Instead, what we have demonstrated is that slightly away from bulk coexistence short-range critical wetting can preserve all its qualitative features when weak long-range forces favouring wetting are included. If we increase a_3 the first-order character of the wetting transition at bulk coexistence becomes stronger, resulting in a longer prewetting line off of coexistence. We then find a first-order prewetting transition instead of a continuous one.

In closing this subsection we calculate the exponent α_s associated with the spreading coefficient for the continuous prewetting transition, following the new approximation for off-of coexistence systems developed in Section 4, Cases 2 and 3 (continuous wetting transitions). The result is $\alpha_s = 0.18 \pm 0.1$, which is in fair agreement with the value 0 expected for short-range critical wetting, and in reasonable agreement with the experimentally determined value -0.22 ± 0.27 .

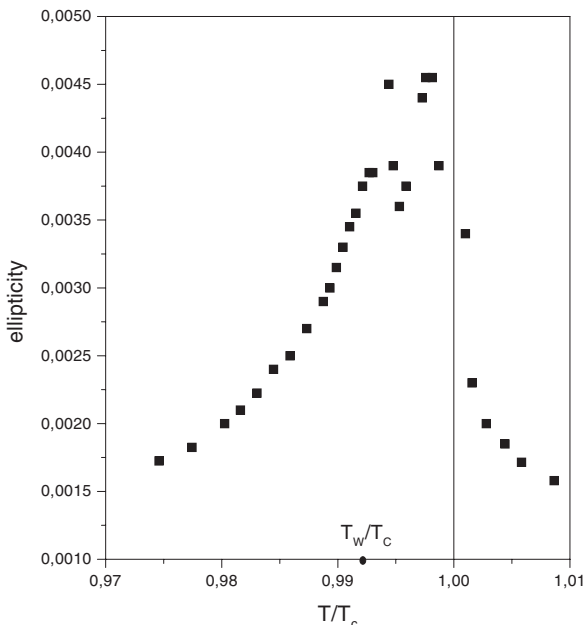


Fig. 12. Experimentally measured ellipticity versus temperature, which is proportional to the adsorption, for the nonane/methanol mixture. The signal is qualitatively the same as in the theoretical Fig. 11. The small dip in the data between wetting and critical adsorption is within the range of the experimental noise.

5.2. Decane/Methanol

For an alkane chain length of 10 the bulk and surface field values are changed slightly with respect to the foregoing case. Using the approximation (5.12) only the molecular weight of the alkane (for decane $m_A = 142.28$ amu) and the upper consolute temperature (for decane/M, $T_c = 364$ K) undergo small changes, leading to the estimate $h = -0.893 \times 10^{-6}$ for decane/methanol. The surface field depends on the difference between $\epsilon_{AA}/k_B = 464$ K and $\epsilon_{MM}^S/k_B = 417$ K, where the superscript S refers to the Stockmayer potential, and we obtain $h_1 = 0.0323$.

Concerning the surface coupling enhancement, we first estimate the K_c value from experimental data for the decane/methanol interfacial tension at ambient temperature. Kahlweit *et al.*⁽³²⁾ provided the measured value 1.93×10^{-3} N/m, while Carrillo *et al.*⁽³¹⁾ obtained about 1.71×10^{-3} N/m. Taking as representative diameter the arithmetic mean of $\sigma_M = 3.65$ Å and $\sigma_A = 6.22$ Å based on the van der Waals equation of state with

$T_c^{\text{LG}} = 617$ K and $P_c^{\text{LG}} = 21.1 \times 10^5$ Pa for decane, we get $\sigma \approx 4.94$ Å. This leads to the two estimates for the dimensionless interfacial tension: $\gamma_{MA} = 0.0938$ and 0.0831 , respectively. Using (3.10) we obtain $c = 0.607$ and 0.538 , respectively, and hence $K_c = 0.184$ and 0.145 . Since the average of these two estimates is only 1% away from $1/6$, it is appropriate to assume also for this system the simple cubic lattice in the MF model description. We conclude $g = -1/6$ as for nonane/methanol.

As for the previous mixture, in the short-range-forces theory the wetting tricritical point for $g = -1/6$ lies at $\phi_0 = 0.5$ according to (4.1), and $h_1 = 0.083$ in view of (4.16). Since the surface field $h_1 = 0.0323$ is smaller than this tricritical value, the predicted short-range wetting transition is critical. It takes place at $\phi_{0,w} = -h_1/g = 0.194$, which corresponds to $T_w/T_c = 0.988$. This is larger than the experimentally determined transition temperature $T_w/T_c = 0.955$, but we have to keep in mind that agonistic LRF will lower the wetting temperature. From (4.1) we obtain $\kappa = -5.15$, which is still well within the critical wetting regime but closer to tricriticality than the previous mixture. For comparison, we recall that the value of κ predicted by the SRF theory when the experimental wetting temperature is used as input is also in the critical wetting regime but much closer to the tricritical value -2 . Table I (for decane and the SC lattice) illustrates this.

The addition of weak long-range forces, for which, for simplicity, we assume the same strength $a_3 = 0.003$, drives the transition very weakly first-order in this theory, as is demonstrated by the remarkable adsorption plot in Fig. 13. The wetting temperature is only slightly lowered to $T_w/T_c = 0.985$, which is not enough to obtain good agreement with the experimental results. Again, we can at best hope to get qualitative agreement using the LRF as a weak perturbation only. The similarity of the adsorption curve of Fig. 13 and the typical vertical tricritical wetting adsorption signal (Fig. 5, curve tcw) is striking. There is hardly a way to distinguish the tricritical adsorption jump from a genuine weak first-order jump of the order parameter. The hysteresis is so minute that the lower and upper spinodal points SP_l and SP_u practically coincide in temperature.

The physics contained in Fig. 13 can be understood in detail by unraveling the wetting phase diagram associated with these SRF and LRF parameters for decane/methanol. This is done in Fig. 14, which shows a clear first-order wetting transition at bulk coexistence, with a first-order prewetting line emerging from it. The lower and upper spinodal lines merge with this prewetting line at the *prewetting critical point*. For bulk fields larger in magnitude than the value associated with this point, the transition is “supercritical” and has the appearance of critical wetting as is the case in Fig. 11 (nonane/methanol). For smaller fields in magnitude the transition is first-order. In the immediate vicinity of the prewetting critical point,

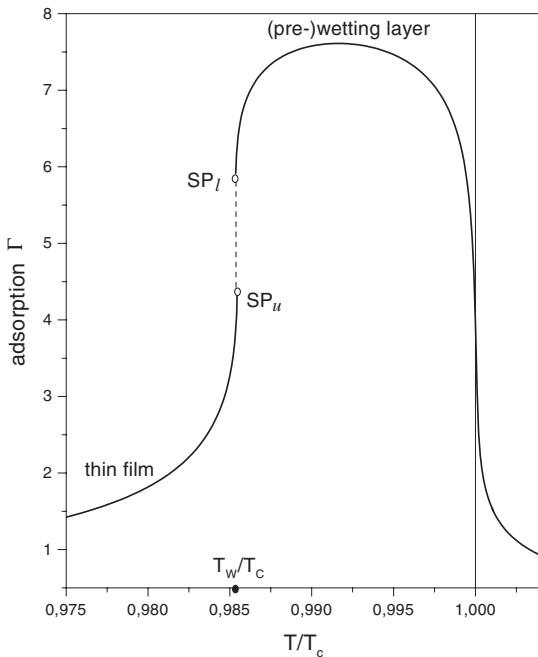


Fig. 13. Adsorption of the methanol-rich phase versus temperature for the model system representing the decane/methanol binary liquid mixture at the liquid-vapour interface. The model parameters bulk field, surface field and surface coupling enhancement are given in the text. The amplitude of the long-range forces favouring wetting has been chosen to be very small, treating these forces as a weak perturbation. Note the very steep and almost continuous wetting signal at $T_w/T_c \approx 0.986$ and the critical adsorption near T_c . The (pre-)wetting transition is of first-order, but very weakly so. The lower and upper spinodal points are also indicated, together with the small jump (dashed line) of the equilibrium order parameter. The system is very close to the prewetting critical point.

relevant to decane/methanol in our approximation of weak LRF, the transition appears tricritical. The adsorption curve of Fig. 13 corresponds to the temperature scan along the dashed line in Fig. 14. The approximate locations of the wetting transition and of the prewetting critical point are indicated by open squares.

It is interesting to examine how the prewetting line meets the bulk coexistence line $h = 0$. The two lines meet tangentially⁽⁴⁵⁾ in a manner governed by the crossover exponent Δ_c ,⁽⁴⁶⁾

$$h \propto (T - T_w)^{\Delta_c}, \quad (5.13)$$

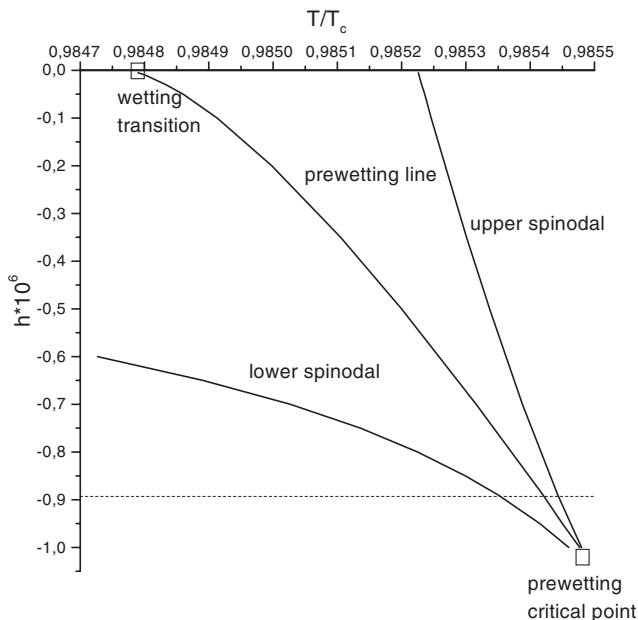


Fig. 14. Wetting phase diagram for the decane/methanol system in the variables bulk field and temperature. The first-order wetting transition at bulk coexistence ($h = 0$) is accompanied by the prewetting line, ending in the prewetting critical point. The lower and upper spinodal lines which merge at this point are also shown. The dashed line gives the temperature scan corresponding to Fig. 13, for the fixed bulk field appropriate to the gravity-induced undersaturation in this system. It should be stressed that the prewetting line is very short, both in h and in T/T_c . Incidentally, the short-range critical wetting point lies at $T/T_c \approx 0.988$ (which is outside the range shown).

with $\Delta_c = 3/2$ for non-retarded van der Waals forces. Indeed, our best fit of the numerical data close to T_w leads to the estimate $\Delta_c = 1.51 \pm 0.01$ and $T_w/T_c \approx 0.98477$. This clearly shows that the van der Waals tails of the net forces between interfaces govern the divergence of the wetting layer thickness and the surface free-energy singularity close to T_w and for $h \rightarrow 0$. For prewetting in systems with short-range forces we would have $\Delta_c = 1$ and in addition a logarithmic correction factor would be present.

The experimental adsorption data for decane/methanol are shown in Fig. 15. The data show a rapid continuous rise, but accompanied by some hysteresis, suggesting that the transition possesses features of both continuous and first-order character. The obvious presence of metastability (in the experimental data) provides fairly strong evidence for an essentially first-order wetting transition.

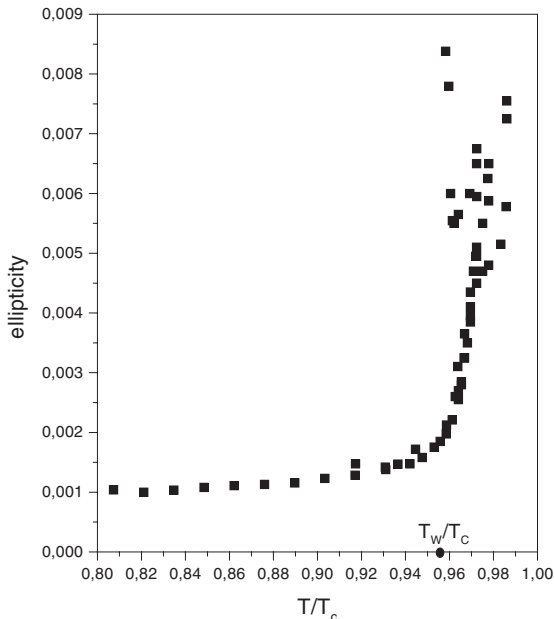


Fig. 15. Experimentally measured ellipticity versus temperature, which is proportional to the adsorption, for the decane/methanol mixture. Besides a continuous variation, reminiscent of critical wetting, also hysteresis has been observed, indicating the first-order character of the transition.

For the critical exponent α_s our fit to the theoretical curve of Fig. 13 for temperatures below and close to T_w gives 0.45 ± 0.1 which compares favourably with the tricritical value $1/2$ and less well with the critical value 0 associated with prewetting criticality (which is just a MF critical point in our model). The experimental estimate for this system is $\alpha_s = 0.68 \pm 0.09$. We conclude that although the transition is, strictly speaking, a first-order transition the exponent α_s is not far from its tricritical value. This is also the case for the experimental system.

5.3. Undecane/Methanol

For this system the bulk field determination proceeds like in the previous ones, taking into account the molecular weight for undecane $m_A = 156.30$ amu and the consolute point for undecane/methanol, $T_c = 376$ K. We obtain $h = -0.974 \times 10^{-6}$. For the surface field we use $\epsilon_{AA}/k_B = 479$ K for undecane, and get $h_1 = 0.0414$.

Concerning the surface coupling enhancement we examine the published experimental results for the undecane/methanol interfacial

tension, as obtained by Carrillo *et al.*⁽³¹⁾ at 298 K. This gives 2.01×10^{-3} N/m. Taking as representative diameter the arithmetic mean of $\sigma_M = 3.65$ Å and $\sigma_A = 6.44$ Å based on the van der Waals equation of state with $T_c^{\text{LG}} = 639$ K and $P_c^{\text{LG}} = 19.7 \times 10^5$ Pa for undecane, we get $\sigma \approx 5.05$ Å. The dimensionless interfacial tension which results after division by $k_B T_c$ and multiplication by σ^2 is $\gamma_{MA} = 0.0988$, implying $c = 0.523$ and hence $K_c = 0.137$. Alternatively, we can interpolate between the data from Kahlweit *et al.*⁽³²⁾ for chain lengths 10 and 12 and use the experimental value 2.31×10^{-3} N/m, or, in dimensionless units $\gamma_{MA} = 0.1133$, so that $c = 0.600$ and $K_c = 0.180$. The average of these two values, $K_c \approx 0.158$ is only 5% away from $1/6$, so that also in this case it is justified to assume the SC lattice to work with, and to set once again $g = -1/6$ for the surface coupling enhancement.

As for the previous mixtures, the short-range-forces theory places the wetting tricritical point for $g = -1/6$ at $\phi_0 = 0.5$ according to (4.1), and $h_1 = 0.083$ in view of (4.16). Since the surface field $h_1 = 0.0414$ is smaller, the short-range wetting transition is critical. It takes place at $\phi_{0,w} = -h_1/g = 0.248$, which corresponds to $T_w/T_c = 0.979$. This is larger than the experimentally determined transition temperature $T_w/T_c = 0.903$, which is consistent with the anticipation that agonistic LRF will lower the wetting temperature. However, since we take the LRF into account only perturbatively, we cannot expect that T_w will be lowered sufficiently to obtain good agreement with experiment. From (4.1) we obtain $\kappa = -4.03$, which is still well within the critical wetting regime but closer to tricriticality than the two previous mixtures. Note that this self-consistent determination of κ differs significantly from the κ presented in Table I for *n*-undecane/methanol (SC lattice), derived using the experimental wetting temperature as input. Indeed, while the latter indicates that the short-range wetting transition is already of first order ($\kappa > -2$), the current self-consistent calculation requires the intervention of the long-range forces to drive the wetting transition first-order.

Weak long-range forces, for which for simplicity we assume the same strength $a_3 = 0.003$ as for both previous mixtures, already drive the transition clearly first-order, as is shown through the adsorption displayed in Fig. 16. The wetting temperature is only slightly lowered to $T_w/T_c = 0.976$, due to the fact that our approach treats the LRF as a small perturbation only. The adsorption curve of Fig. 16 differs somewhat from the typical first-order adsorption signal (Fig. 2) in that the hysteresis is much smaller. This is due to the vicinity of the system to the prewetting critical point. Interestingly, the experimental data for this mixture displayed in Fig. 17 show a clear first-order jump but without hysteresis, unlike for decane/methanol. The fact that the hysteresis is unobservably small is in line with

recent experiments on other binary liquid mixtures, such as cyclohexane/ CD_3OD with gravity-thinned wetting layers not thicker than about 100 \AA .⁽⁴⁷⁾ In contrast, in almost density-matched systems, like cyclohexane/methanol, with gravity-thinned wetting layers of about 400 \AA , much larger hysteresis is observed. This has now been understood by calculating the activation energy for wetting layer nucleation as a function of the film thickness.⁽⁴⁷⁾ Therefore, the surprising feature is not the absence of hysteresis for undecane/methanol, but the presence of it for decane/methanol!

Finally, obviously for this fairly strong first-order wetting transition the critical exponent analysis immediately leads to $2 - \alpha_s = 1$, as expected, since the mean-field free-energy branches cross, leading to a corner in the equilibrium free energy (discontinuous derivative).

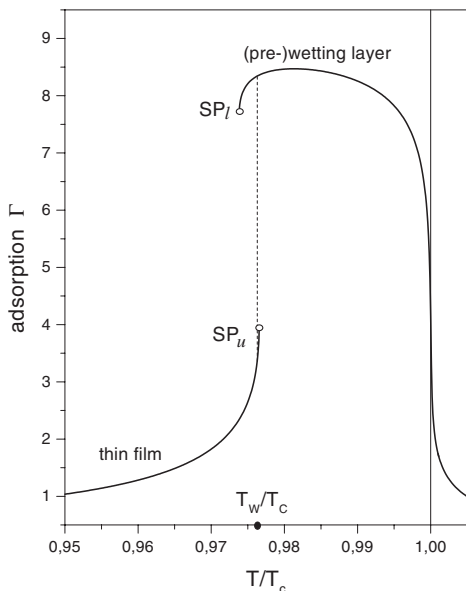


Fig. 16. Adsorption of the methanol-rich phase versus temperature for the model system representing the undecane/methanol binary liquid mixture at the liquid-vapour interface. The model parameters bulk field, surface field and surface coupling enhancement are given in the text. The amplitude of the long-range forces favouring wetting has been chosen to be very small, treating these forces as a weak perturbation. Note the clear first-order (pre)wetting transition at $T_w/T_c \approx 0.976$ and the critical adsorption at T_c . The lower and upper spinodal points are also indicated, together with the jump (dashed line) of the equilibrium order parameter. The hysteresis is quite small.

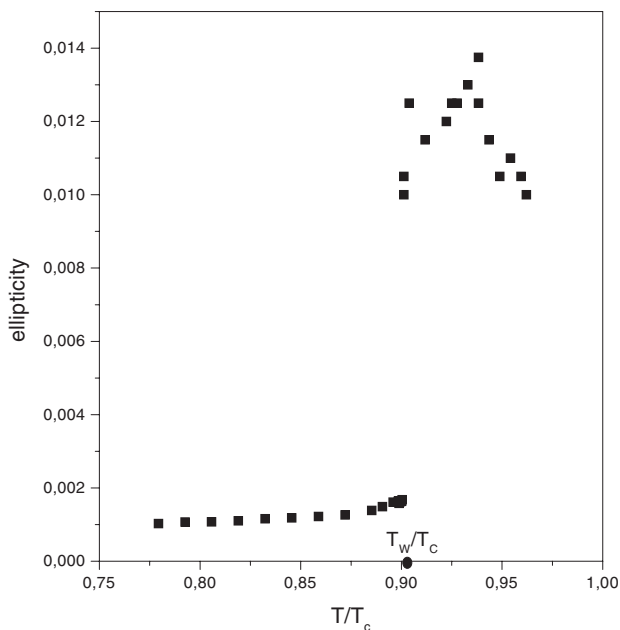


Fig. 17. Experimentally measured ellipticity versus temperature, which is proportional to the adsorption, for the undecane/methanol mixture. A clear first-order transition is seen. However, no hysteresis is observed.

6. CONCLUSIONS

In this paper we have been concerned with addressing theoretically a variety of recently observed wetting phenomena displaying the richness of the wetting phase diagram proposed by Nakanishi and Fisher,⁽²²⁾ featuring first-order, critical and tricritical wetting. In addition, we have studied how, for the experimental systems under consideration, the wetting phase transitions are modified by taking into account approximately the effect of long-range forces. Many authors, in particular de Gennes, and Ebner and Saam, predicted that for long-range forces favouring wetting, critical wetting transitions should become first-order.^(4,11) This is not what is observed in the experiments. Mixtures of alkanes and methanol, with the methanol-rich phase wetting the liquid-vapour interface, have been observed to pass from continuous wetting to first-order wetting as the alkane chain length is increased from 9 till 11. The experiments are consistent with a tricritical wetting transition occurring at some intermediate effective chain length between 9.6 and 10.⁽³⁵⁾

The theoretical description which we have explored here supplements previous works on similar systems in two respects: we have taken into account that the systems are *slightly away from the conditions of bulk two-phase coexistence*, and, more importantly, we have allowed for *effects of long-range forces between interfaces*, arising from the inverse power-law van der Waals forces between the molecules.

It has been necessary to make these extensions of the theory, simply because several paradoxes concerning the interpretation of the experiments were up to now left unresolved. For example, the main apparent contradiction embodied in the observation of short-range critical wetting^(1,2) is that *van der Waals forces favouring wetting should drive the transition first-order*. Why was this not seen in the experiments? The answer that we provide here, and which is complementary to the points of view defended in refs. 1 and 2, is that weak long-range forces *combined with* a small “bulk field” which takes the phases just slightly off of coexistence, do not alter the appearance of short-range critical wetting.

We have thus obtained evidence that on the one hand critical wetting can persist, to any reasonable degree of computational accuracy or practical observability, in slightly undersaturated systems with weak long-range forces favouring wetting, while on the other hand first-order wetting is—of course—the generic phenomenon. Consequently, it is fundamentally interesting to scrutinize the cross-over between the two. The experiments have shown⁽³⁵⁾ that this cross-over is consistent with a short-range tricritical wetting transition scenario. Here we find that this interpretation is a good approximation, adequate for all practical purposes, even in systems which instead of displaying strict tricriticality, show a very short prewetting line emerging from a first-order wetting transition at bulk coexistence. The role of the tricritical point in the short-range forces limit is taken over by that of the prewetting critical point in the presence of agonistic long-range forces, no matter how weak. The two are difficult to distinguish in practice, both as regards the order parameter singularity and concerning the critical exponent associated with the surface free energy singularity. This exponent, α_s , takes the value 1/2 for tricritical wetting and the value 0 for prewetting criticality.

In sum, systems slightly off of coexistence can behave qualitatively differently from those at coexistence. The most spectacular example we have found in this regard is the possibility of a continuous-looking wetting transition under circumstances in which the wetting transition at coexistence is always of first order. This is the case when the long-range forces are agonistic, and consequently short-range first-order wetting remains first-order, and short-range critical wetting must turn into a first-order transition, in principle.

The methods we have employed and the theory we have developed are to a large extent qualitative, at times heuristic, and eventually amount to a simple mean-field description of the interacting many-body system. Why should the mean-field theory be a good approximation in this case? There are several justifications, the most decisive of which is that the width of the critical region in which deviations from mean-field critical behaviour should occur is far too small to be observable experimentally or in Monte Carlo simulations for equivalent Ising-like systems with short-range forces. This is a prediction from the latest sophisticated functional Renormalization Group theory. The second reason is that, as soon as van der Waals forces are added to the theory, the upper critical dimension above which mean-field critical exponents are valid, is lowered from $d_u = 3$ (short-range forces) to $d_u < 3$. The third reason is the clarity of the investigation. We have included the effect of a small bulk field, and of a weak substrate-adsorbate field with algebraic decay, as complications on top of an otherwise already rich Cahn–Landau theory. It would not be instructive to add yet a third complication, in the form of forces arising from interface capillary wave fluctuations, before a full understanding of the other two refinements has been achieved. Moreover, due to the undersaturation of the wetting phase (gravitational thinning of the wetting layer) the parallel and transverse correlation lengths of the relevant unbinding interface cannot get large enough for long-wavelength capillary waves to develop. So the presence of the bulk field renders capillary-wave considerations superfluous, at least in this system.

While adhering fully to a mean-field theory, we have also indicated how one can arrive at the surface free-energy functional starting from a microscopic lattice model of Ising spin-1 type. Further, we have aimed at providing reasonable estimates for all the phenomenological parameters in the theory, starting from microscopic system constants such as molecular interaction potentials (pair energies and particle diameters) and molecular weights. In this way the bulk field, surface field and surface enhancements appropriate to the different mixtures have been related to more fundamental variables. It has not been possible to complete this scheme fully self-consistently, and it has been necessary to use as input experimentally measured interfacial tensions, for example, for obtaining the appropriate lattice coordination number in the microscopic model, leading to the use of a simple cubic lattice.

The important parameter for which we have been unable to provide a reliable system-specific estimate is the amplitude a_3 of the long-range forces. The reason for this is that the theory requires the knowledge of the entire function $h(z)$ while only the leading term, related to the Hamaker constant, is known with reasonable accuracy for a given system. To resolve

this draw-back, we have opted for a perturbative theory, in which the effect of weak long-range forces is examined on the wetting transitions dictated by the theory incorporating short-range forces. We have thus fixed a_3 to a value, one order of magnitude smaller than an estimate based on the Hamaker constant. This is in line with the experimental fact that the physics predicted by the theory involving short-range forces is in good accord with the observed continuous wetting phenomenon in nonane/methanol.^(1,2) The most remarkable of our findings is that the long-range forces *are* perturbative. Indeed, the inclusion of weak long-range forces does *not* turn the observable critical wetting transition into a first-order one. This seemingly contradicts previous theoretical works which indicated that critical wetting must be ruled out for agonistic LRF. As we emphasized, this is due to the presence of a small bulk field, turning macroscopic wetting layers into mesoscopic ones (only hundreds of Å thick).

As new technical theoretical advances we have achieved the computation of generalizations of spreading coefficients for systems slightly displaced from two-phase coexistence in bulk. This is useful for continuous wetting transitions, in the vicinity of which only one surface state is thermodynamically stable. Further, we have found that the adsorption is on many accounts a useful and well-defined order parameter, which is easy to interpret, in contrast with the wetting layer thickness. Using the adsorption the phenomena of (pre-)wetting and critical adsorption can be viewed on equal footing (see Figs. 2, 5, 11, 13, and 16) and comparison with the experimentally measured ellipticity is directly possible.

All in all, we believe that the present work elucidates the systems in as far as mean-field theory can describe them. The additions of deviations from bulk coexistence and the perturbative effect of long-range forces appear crucial to a better modeling and understanding of the experiments.

ACKNOWLEDGMENTS

We thank Michael Fisher, Peter Monson, Peter Nightingale, Thanassos Panagiatopoulos, J. I. Siepmann, and Ben Widom for advice concerning the determination of the mixed pair energy ϵ_{AB} . We further thank Emanuel Bertrand and Denis Fenistein for discussions and communicating unpublished results. We are also grateful to Christopher Boulter, Siegfried Dietrich and the referees for suggesting improvements of the presentation. This research is supported by the Inter-University Attraction Poles and the Concerted Action Programme. A.I.P. is KULeuven Junior Fellow under contract OF/99/045 and F/01/027. LPS de l'ENS is UMR 8550 of the CNRS, associated with the Universities Paris 6 and 7. This research has

been supported in part by the European Community TMR Research Network "Foam Stability and Wetting", contract nr FMRX-CT98-0171, and by the NRC/NIST postdoctoral research program.

REFERENCES

1. D. Ross, D. Bonn, and J. Meunier, *Nature* **400**:737 (1999).
2. D. Ross, D. Bonn, and J. Meunier, *J. Chem. Phys.* **114**:2784 (2001).
3. D. Bonn and D. Ross, *Rep. Prog. Phys.* **64**:1085 (2001).
4. P. G. de Gennes, *C. R. Acad. Sc. Paris* **297**:9 (1983).
5. M. P. Nightingale, W. F. Saam, and M. Schick, *Phys. Rev. Lett.* **51**:1275 (1983); *Phys. Rev. B* **30**:3830 (1984).
6. V. Privman, *J. Chem. Phys.* **81**:2463 (1984).
7. M. P. Nightingale and J. O. Indekeu, *Phys. Rev. B* **32**:3364 (1985).
8. D. M. Kroll and T. F. Meister, *Phys. Rev. B* **31**:392 (1985).
9. S. Dietrich and M. Schick, *Phys. Rev. B* **31**:4718 (1985); *Phys. Rev. B* **33**:4952 (1986).
10. C. Ebner, W. F. Saam, and A. K. Sen, *Phys. Rev. B* **32**:1558 (1985).
11. C. Ebner and W. F. Saam, *Phys. Rev. B* **35**:1822 (1987); *Phys. Rev. Lett.* **58**:587 (1987); *Phys. Rev. B* **37**:5252 (1988).
12. T. Getta and S. Dietrich, *Phys. Rev. E* **47**:1856 (1993).
13. K. Ragil, J. Meunier, D. Broseta, J. Indekeu, and D. Bonn, *Phys. Rev. Lett.* **77**:1532 (1996).
14. E. Brézin, B. I. Halperin, S. Leibler, *Phys. Rev. Lett.* **50**:1387 (1983); *J. Phys. (France)* **44**:775 (1983); R. Lipowsky, D. M. Kroll, and R. K. P. Zia, *Phys. Rev. B* **27**:4499 (1983).
15. D. S. Fisher and D. A. Huse, *Phys. Rev. B* **32**:247 (1985).
16. M. E. Fisher and A. J. Jin, *Phys. Rev. Lett.* **69**:792 (1992).
17. C. J. Boulter, *Phys. Rev. Lett.* **79**:1897 (1997).
18. K. Binder, D. P. Landau, and D. M. Kroll, *Phys. Rev. Lett.* **56**:2272 (1986).
19. C. J. Boulter and A. O. Parry, *Phys. Rev. Lett.* **74**:3403 (1995).
20. A. O. Parry and C. J. Boulter, *Phys. Rev. E* **53**:6577 (1996).
21. A. O. Parry and P. Swain, *Phys. A* **250**:167 (1998).
22. H. Nakanishi and M. E. Fisher, *Phys. Rev. Lett.* **49**:1565 (1982).
23. J. M. Yeomans, *Statistical Mechanics of Phase Transitions*, Chap. 3 (Clarendon Press, Oxford, 1992).
24. S. Dietrich and A. Latz, *Phys. Rev. B* **40**:9204 (1989).
25. R. C. Reid and T. K. Sherwood, *The Properties of Gases and Liquids* (McGraw-Hill, New York, 1966).
26. A. Maritan, G. Langie, and J. O. Indekeu, *Physica A* **170**:326 (1991).
27. J. W. Cahn, *J. Chem. Phys.* **66**:3667 (1977).
28. J. N. Israelachvili, *Intermolecular and Surface Forces* (Academic Press, London, 1992).
29. J. S. Rowlinson, *Liquids and Liquid Mixtures* (Butterworth, London, 1969).
30. J. O. Indekeu, *Acta Phys. Polonica B* **26**:1065 (1995). For a summary, see J. O. Indekeu, *Physica Scripta* **T35**:31 (1991).
31. E. Carrillo, V. Talanquer, and M. Costas, *J. Phys. Chem.* **100**:5888 (1996). For studies of the interfacial tension near consolute points of binary liquid mixtures, see H. Chaar, M. R. Moldover, and J. W. Schmidt, *J. Chem. Phys.* **85**:418 (1986).
32. M. Kahlweit, G. Busse, D. Haase, and J. Jen, *Phys. Rev. A* **38**:1395 (1988).
33. D. Y. Peng and D. B. Robinson, *Ind. Eng. Chem. Fundamentals* **15**:59 (1976).

34. J. H. Sikkenk, J. O. Indekeu, J. M. J. van Leeuwen, and E. O. Vossnack, *Phys. Rev. Lett.* **59**:98 (1987).
35. D. Ross, D. Bonn, A. I. Posazhennikova, J. O. Indekeu, and J. Meunier, *Phys. Rev. Lett.* **87**:176103 (2001).
36. J. O. Indekeu, K. Ragil, D. Bonn, D. Broseta, and J. Meunier, *J. Stat. Phys.* **95**:1009 (1999).
37. See, for example, D. Bonn, Ph.D. thesis, Universiteit van Amsterdam, 1993.
38. R. Blossey and C. Oligschleger, *J. Colloid Interface Sc.* **209**:442 (1999).
39. R. Blossey, *Int. J. Mod. Phys. B* **9**:3489 (1995).
40. M. E. Fisher and P. G. de Gennes, *C. R. Acad. Sci. Ser. B* **287**:207 (1978); A. J. Liu and M. E. Fisher, *Phys. Rev. A* **40**:7202 (1989).
41. A. Maciolek, A. Ciach, and R. Evans, *J. Chem. Phys.* **108**:9765 (1998); A. Drzewinski, A. Ciach, and A. Maciolek, *Eur. Phys. J.* **B5**:825 (1998).
42. P. G. de Gennes, *J. Physique (Lett)* **42**:L377 (1981).
43. S. Dietrich and M. Napiorkowski, *Phys. Rev. A* **43**:1861 (1991).
44. D. Bonn, E. Bertrand, N. Shahidzadeh, K. Ragil, H. T. Dobbs, A. I. Posazhennikova, D. Broseta, J. Meunier, and J. O. Indekeu, *J. Phys. Condens. Matter* **13**:4903 (2001).
45. E. H. Hauge and M. Schick, *Phys. Rev. B* **27**:4288 (1983).
46. For details on the singular behaviour of various thermodynamic quantities at first-order wetting, see, for example, J. O. Indekeu, *Int. J. Mod. Phys. B* **8**:309 (1994).
47. D. Bonn, E. Bertrand, J. Meunier, and R. Blossey, *Phys. Rev. Lett.* **84**:4661 (2000).